molecular pharmaceutics

Review

pubs.acs.org/molecularpharmaceutics

Nanotheranostics of Circulating Tumor Cells, Infections and Other Pathological Features *in Vivo*

Jin-Woo Kim,*[,†,‡,§] Ekaterina I. Galanzha,[∥,⊥] David A. Zaharoff,[§] Robert J. Griffin,[⊥,#] and Vladimir P. Zharov*[,∥,⊥]

[†]Bio/Nano Technology Laboratory, Institute for Nanoscience and Engineering, [‡]Department of Biological and Agricultural Engineering, and [§]Department of Biomedical Engineering, University of Arkansas, Fayetteville, Arkansas 72701, United States

[∥]Phillips Classic Laser and Nanomedicine Laboratories, [⊥]Arkansas Nanomedicine Center, and [#]Department of Radiation Oncology, University of Arkansas for Medical Sciences, Little Rock, Arkansas 72205, United States

ABSTRACT: Many life-threatening diseases are disseminated through biological fluids, such as blood, lymph, and cerebrospinal fluid. The migration of tumor cells through the vascular circulation is a mandatory step in metastasis, which is responsible for ~90% of cancer-associated mortality. Circulating pathogenic bacteria, viruses, or blood clots lead to other serious conditions including bacteremia, sepsis, viremia, infarction, and stroke. Therefore, technologies capable of detecting circulating tumor cells (CTCs), circulating bacterial cells (CBCs), circulating endothelial cells (CECs), circulating blood clots, cancer biomarkers such as microparticles and exosomes, which contain important microRNA signatures, and other abnormal features such as malaria parasites in biological fluids may facilitate early diagnosis and treatment of metastatic cancers, infections, and adverse cardiovascular events. Unfortunately, even in a disease setting, circulating abnormal cells are rare events that are easily obscured by the overwhelming background material in whole blood. Existing detection methods mostly rely on *ex vivo* analyses of limited volumes (a few milliliters) of blood samples. These small volumes limit the probability of detecting CTCs, CECs, CBCs and other rare phenomena. *In vivo* detection platforms capable of continuously monitoring the entire blood volume may substantially increase the probability of detecting circulating abnormal cells and, in particular, increase the opportunity to identify exceedingly rare and potentially dangerous subsets of these cells, such as circulating cancer stem cells (CCSCs). In addition, *in vivo* detection technologies capable of destroying and/or capturing circulating abnormal cells may inhibit disease progression. This review focuses on novel therapeutic and diagnostic (theranostic) platforms integrating *in vivo* real-time early diagnosis and nano-bubble based targeted therapy of CTCs, CECs, CBCs and other abnormal objects in circulation. This critical review particularly focuses on nanotechnology-based theranostic (nanotheranostic) approaches, especially *in vivo* photoacoustic (PA) and photothermal (PT) nanotheranostic platforms. We emphasize an urgent need for *in vivo* platforms composed of multifunctional contrast nanoagents, which utilize diverse modalities to realize a breakthrough for early detection and treatment of harmful diseases disseminated through the circulation.

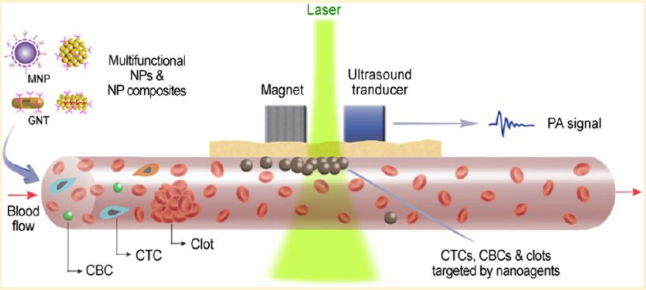

KEYWORDS: *metastasis, circulating tumor cells (CTCs), circulating endothelial cells (CECs), circulating cancer stem cells (CCSCs), circulating microparticles and exosomes, circulating pathogens, viruses and parasites, blood clots, blood and lymph flow, contrast nanoagents, positive and negative photoacoustic contrasts, micro- and nanobubbles, multimodal, multicolor, nanotechnology, multifunctional real-time nanotheranostics, nanomedicine*

■ INTRODUCTION

Progression of many fatal diseases is mediated through the vascular dissemination of pathological cells. For example, tumor cells are continuously shed from primary solid tumors into the vascular circulation. These circulating tumor cells (CTCs) are the precursors of metastasis, which accounts for 9 out of every 10 cancer-related deaths.[1] Also, bacteria reaching the circulation often cause systemic infections and sepsis. Bacteremia is a significant cause of mortality in developing countries as well as a threat to developed countries due to the rapid emergence of antibiotic-resistant strains.[2] Furthermore, arterial and pulmonary embolisms due to circulation of blood clots often lead to severe cardiovascular and cerebrovascular events. Taken together, the detection and enumeration of circulating pathological features, such as CTCs, circulating bacterial cells (CBCs), and clots (referred also as throm-

Special Issue: Theranostic Nanomedicine with Functional Nanoarchitecture

Received: October 11, 2012
Revised: February 1, 2013
Accepted: February 4, 2013
Published: February 4, 2013

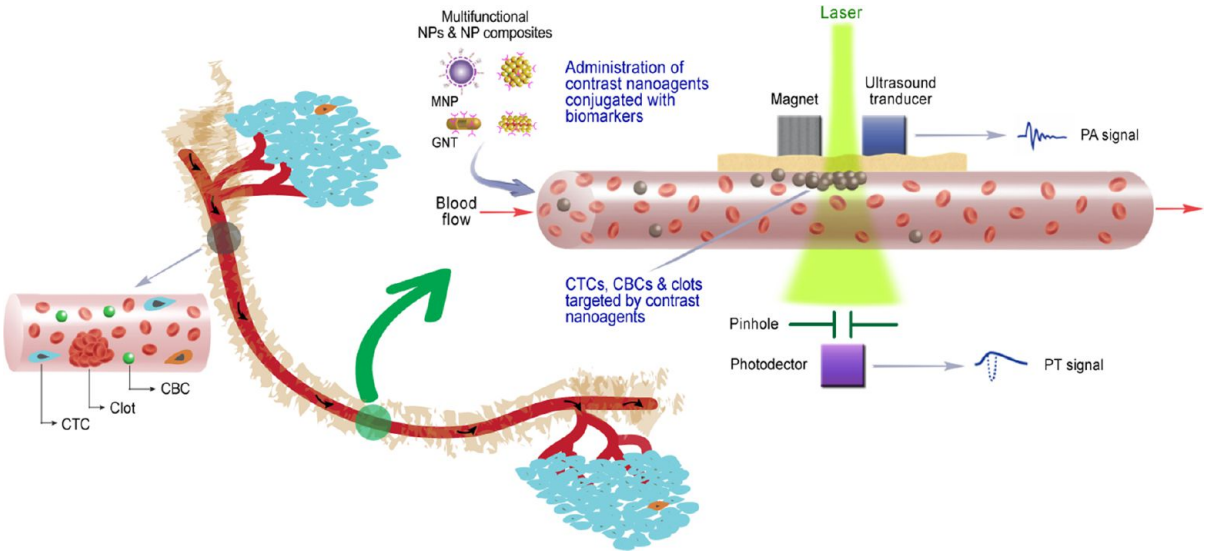

Figure 1. *In vivo* multimodal multicolor nanotheranostic platform integrating magnetic enrichment, PA detection, PT therapy, and real-time PA monitoring of PT therapeutic efficacy of circulating pathological features, including circulating tumor cells (CTCs), circulating endothelial cells (CECs), circulating cancer stem cells (CCSCs), circulating bacterial cells (CBCs), circulating blood clots (i.e., thromboemboli and emboli), and other biomolecules and cells (i.e., DNA, RNA, exosomes and microparticles, parasites, etc.).

boemboli or emboli), are clinically significant for many life-threatening diseases.

However, detection of circulating abnormal features presents numerous challenges given their rarity relative to the overwhelming amount of nonpathogenic or background material in blood. For example, even in patients with advanced cancer, only about one CTC for every million leukocytes and billion erythrocytes is expected. To date, most detection methods enumerate circulating abnormal cells in a small volume (5−20 mL) of blood drawn from patients.[3−15] The small sample volume limits the ability of *ex vivo* techniques to detect exceedingly rare populations. In particular, the potential for real-time diagnosis of metastatic diseases at earlier stages is hindered by low cell counts in small volumes acquired at fixed time points.[11,13] Furthermore, the use of small blood volumes limits the collection of abnormal cells for later analysis to investigate their role in disease progression. Hence, the development of effective and efficient detection platforms capable of interrogating the entire circulation *in vivo* and in real time is necessary to realize the enormous diagnostic potential of circulating pathogenic cells and biomolecules.

Recent development of nanoparticles (NPs) with unique physicobiochemical properties for biomedical applications offers immense promise in the advancement of therapeutics and diagnostics (theranostics). Various NPs with different shapes and compositions have been proven effective as theranostic contrast nanoagents.[9,16−20] Particularly, tunable near-infrared (NIR)-responsive plasmonic NPs, including gold nanoshells (GNSs), gold nanorods (GNRs), and golden carbon nanotubes (GNTs),[9,12,16,21] have attracted attention for minimally invasive imaging and therapy owing to their high NIR absorption (e.g., ∼700−900 nm) in the window of optical transparency of most biological tissues as well as high efficiency conversion of absorbed energy into thermal and acoustic phenomena.[2,9,11−15] Recently,[2,9,11−15] a completely new *in vivo* noninvasive multicolor and multimodal concept using dual NIR-responsive NP-based contrast agents and two-color laser-based *in vivo* photoacoustic (PA) and photothermal (PT) flow cytometry (PAFC/PTFC) to detect, capture, and purge rare circulating tumor and other pathological cells in the peripheral circulation were introduced by our team (Figure 1). These technical platforms demonstrated high potential to overcome the aforementioned limitations of small blood sample volumes and to enable a broad range of clinical applications, including early disease theranostics and evaluation of disease progression.[2,9,11−15] Some groups also proposed similar approaches to achieve real-time detection of CTCs using fluorescence-labeled biomarkers with some degree of success.[22,23] Although PAFC/PTFC is still at an early stage in development, the *in vivo* theranostic platforms, in particular nanotechnology-based theranostics (nanotheranostics), carry enormous clinical potential for the therapy and management of life-threatening diseases.

Here, we review recent advances in *in vivo* real-time detection and characterization of circulating pathogenic cells and other disease-associated features. The challenges of *in vivo* detection, particularly at early stages of disease, are discussed as well as several potential strategies to overcome them. This critical review is not meant to be comprehensive. The history and current state of the art and science for cancer cell metastasis and recent advances in their detection technologies, in particular *ex vivo* approaches and a few reports on *in vivo* micro- or macro-scale devices such as implantable microfluidic devices, have been reviewed elsewhere.[3−7,10] Specifically, this critical review focuses on nanotheranostic approaches, particularly PA and PT *in vivo* platforms, with advanced multifunctional contrast nanoagents to realize real-time imaging and therapy for CTCs and other circulating pathological cells and biomolecules. Also, we stress the need and promise of *in vivo* multimodal synergistic platforms, which integrate multimodal contrast nanoagents and multiple modalities for effective early diagnosis and therapy. Finally, we conclude with a discussion of future directions and current needs for research in the field. The purpose of this discussion is to stimulate ideas regarding practical strategies for implementation of *in vivo* multifunctional nanotheranostics in the clinic.

CHALLENGES AND OPPORTUNITIES

The detection of circulating markers of disease including CTCs, circulating endothelial cells (CECs), circulating cancer stem cells (CCSCs), CBCs, circulating blood clots, and other biomolecules and cells (i.e., DNA, RNA, exosomes, microparticles, parasites and other infected cells) is emerging as a vital clinical tool for the early diagnosis and treatment of cancer, infections, and cardiovascular diseases. In addition, platforms that allow for the collection of sufficient numbers of circulating pathogenic cells are helping to elucidate critical biological mechanisms of disease progression. For example, the collection and study of CTCs is helping improve our understanding of metastasis, including the discovery of critical surface and intracellular biomarkers related to metastatic progression and/or more aggressive phenotypes.

A considerable number of highly sensitive and specific *ex vivo* detection techniques are under investigation to detect CTCs, CECs, and CBCs in small volumes of peripheral blood. These techniques involve reverse transcriptase polymerase chain reaction (RT-PCR), flow cytometry, microfluidics-based technologies, and others.[3−11] The relative ease of sample collection makes *ex vivo* peripheral blood assessments convenient for noninvasive monitoring of disease progression. However, sensitivity thresholds of existing *ex vivo* detection methods are 1−10 cells per 1 mL of whole blood. Therefore, on average, abnormal cells remain undetectable until their numbers reach 5,000−50,000 in an average adult blood volume of ∼5 L.

Another challenge is that CTCs, like many circulating pathogenic cells, are highly heterogeneous.[24−26] Not all CTCs express the same markers, and some may even have completely different phenotypes than the associated primary tumor.[1] Furthermore, while CTCs are mandatory for metastasis, not all CTCs cause metastasis.[24−27] Recent evidence indicates that certain subpopulations of CTCs, such as tumor-initiating cells or CCSCs,[27] may be key drivers of metastasis.[1] In fact, only about 0.01% of CTCs were estimated to form metastatic lesions.[28,29] It is not known whether this 0.01% represents a unique subset of aggressive tumor cells, perhaps CCSCs or invasive mesenchymal-like tumor cells, or whether 0.01% represents the infinitesimal probability that a given CTC can survive a "decathlon"[29] of challenges to establish a metastatic lesion. If 0.01% represents some exceedingly rare subpopulation of CTCs, the probability of detecting or collecting these cells in a 5−20 mL sample is negligible.

Similar to cancer metastasis via CTCs, many key questions regarding bacteria dissemination to distant organs, including CBC migration in tissue, invasion dynamics, interaction with blood and endothelial cells, and extravasation, remain unanswered.[2] Unfortunately, the removal of either CTCs or CBCs from the host in order to study their biological processes may alter properties, such as cell morphology and biomarker expression. Moreover, *in vitro* sample preparation procedures do not reproduce the native *in vivo* environment, and thus are not able to provide accurate data regarding native cell-to-cell interactions, cell migration, or control of cell apoptosis and proliferation by the host environment.[15]

We submit that *in vivo* real-time nanotheranostics has the potential to overcome challenges associated with detecting exceedingly rare populations in whole blood and to help elucidate unknown biological mechanisms of disease progression. Regarding the former, an *in vivo* approach allows for the interrogation of the entire (∼5 L) circulation, which is expected to increase detection sensitivity by at least 2 if not 3 order of magnitude over current *ex vivo* approaches. Regarding the mechanisms of disease progression, *in vivo* nanotheranostics can enrich abnormal cells for either *in vivo* analyses of biological function or minimally invasive extraction to perform assessments *ex vivo*. A third advantage of nanotheranostics is the ability to monitor responses to various therapies continuously and in real time. *Ex vivo* approaches offer only snapshots of responses during treatment. A fourth advantage of *in vivo* nanotheranostics is their potential for delivering treatment or destroying pathogenic cells upon recognition. This targeted elimination of pathogenic cells may significantly alter the course of disease.

We note that, even with increased specificity and the capability to do continuous monitoring, the markers and targets allowing us to identify these rare events are still under exploration. As discussed later, few if any validated targets have been identified. Nonetheless, *in vivo* real-time nanotheranostics, with the advent of more reliable detection markers, represent a potentially powerful tool for early detection and management of life-threatening diseases. Subsequent sections of this review will cover recent advances, technical challenges, and strategies for future development.

IN VIVO NANOTHERANOSTICS OF CIRCULATING DISEASE-ASSOCIATED CELLS AND BIOMOLECULES: RECENT ADVANCES

In this section, we present the current status of *in vivo* nanotheranostic platform development for circulating disease-associated cells and biomolecules. In particular, we focus on *in vivo* PAFC/PTFC nanotheranostic platforms with advanced contrast nanoagents. It is noted that a similar approach using fluorescence-labeled tumor-associated ligands for *in vivo* FC is also under investigation.[22,23,30] However, *in vivo* applications using fluorescent labels are usually hampered by tag-associated problems such as photobleaching, blinking or strong light scattering, and background autofluorescence.[11] On the other hand, contrast nanoagents, such as plasmonic nanoparticles, exhibit much higher optical absorption and photostability. Furthermore, when integrated with PA and PT techniques, nanoagents are capable of multimodal detection and therapy of abnormal cells.

***In Vivo* PAFC and PTFC Nanotheranostic Platform.** *In vivo* real-time PAFC/PTFC detection of circulating abnormal cells and biomolecules using NIR NPs as PA and PT contrast agents was first demonstrated in 2004 by Zharov et al.,[31] followed by its further development and extension to various biomedical applications.[2,9,11−16,30−44] In 2009, our group reported a novel multicolor PAFC/PTFC using novel multimodal NPs as nanotheranostic agents and demonstrated, for the first time, *in vivo* real-time imaging and therapy of CTCs and CCSCs.[9,11−15] Other theranostic targets, including bacteria (i.e., CBCs), micro/nanoparticles, and emboli,[9,11] were also explored. In these studies, we demonstrated the potential of *in vivo* multispectral PAFC/PTFC for ultrasensitive noninvasive molecular quantitative detection, intravascular magnetic enrichment, and targeted laser ablation of pathological cells in circulation. The multicolor multiparameter high-speed PAFC/PTFC was capable of clinically relevant molecular detection and enumeration of cells of interest among highly heterogeneous populations of blood cells *in vivo* that has never been possible before. Integration of PA and PT

approaches using the same technical platform allowed robust and relatively inexpensive combination of diagnosis and targeted therapy of rare abnormal cells directly in blood circulation *in vivo*. The potential advantages of PAFC/PTFC in comparison with other *in vitro* approaches include (1) analyzing mobile cells in moving fluids, (2) rapid (a few minutes) testing (up to $\sim 10^{11}$ cells/s in human jugular vein) of the largest blood volume (up to whole blood volume, i.e., ~50−100 times more than the volume of conventional samples) at unrestricted speeds, and (3) unprecedented sensitivity threshold at one pathological cell, such as a CTC, among a billion normal blood cells and millions of white blood cells (WBCs) in lymph flow.[11,36] The advantages of PAFC over existing *in vivo* technologies also include (1) time-resolved and deep detection of specific acoustic signals from individual metastatic cells (depth up to 7 cm), (2) multicolor detection, (3) use of functionalized NPs as unique NIR-absorbing low toxic supercontrast PA molecular agents, and (4) noninvasiveness for normal tissue due to a relatively low level of laser energy, i.e., well within safety parameters of laser use for humans.

PAFC/PTFC Schematics. The nanotheranostic platform integrates *in vivo* PAFC/PTFC and PT therapy of circulating abnormal objects, e.g., CTCs, CBCs, etc. (Figure 1).[9,11−13] PAFC is based on time-resolved detection of laser-induced acoustic waves from targeted objects (referred to as PA signals) with an ultrasound transducer attached to the skin (Figure 1). Laser radiation can be delivered to biological tissue by using either a microscope schematic with a customized condenser to create the desired linear beam shapes ranging from 5 × 50 μm to 25 × 150 μm or a fiber with a miniature tip and cylindrical optics. PAFC molecular specificity is provided either by label-free intrinsic absorption spectroscopic contrast (e.g., hemoglobin or melanin) or by strongly absorbing, low-toxicity, biofunctionalized contrast nanoagents, such as NPs. Preclinical feasibility studies of PAFC and PTFC *in vivo* involved nude mouse tumor models of melanoma (Figure 2A) and breast cancer (Figure 2B). The noninvasive

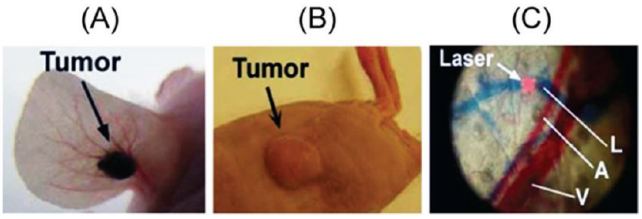

Figure 2. Animal models. (A) Mouse ear melanoma model. (B) Mouse breast cancer model. (C) Ear fragment (A, arteriole; V, vein; and L, lymph) visualized with Evans Blue staining *in vivo*.

PA detection of cells in blood and lymphatic systems was carried out using (1) the mouse ear (Figure 2C) and (2) the skinfold chamber.

The use of a single technique limits the range of detectable cells with different optical properties.[11] Recently, we demonstrated real-time integration of PAFC and fluorescent flow cytometry (FFC), termed PAFFC,[30] using pulsed and continuous wave (CW) lasers as traditional sources for the generation of PA and fluorescent signals, respectively. Conventional PA and fluorescence techniques use preferential positive imaging contrasts when signals from strongly absorbing or fluorescent cells are above absorption or autofluorescence background, respectively. In PAFFC, conventional positive contrast mode was combined with the new negative PA and fluorescent contrast modes especially for PA detection of cells with lower absorption than red blood cells (RBCs) similarly as platelets or WBCs.[42] PAFC was also integrated with PT techniques, i.e., PTFC and PT therapy.[9,11,16,32] In the diagnostic mode with PT thermal lens, a laser-induced refractive heterogeneity causes defocusing of a collinear He−Ne laser probe beam and hence a reduction in the beam's intensity at its center, as detected by a photodiode with a pinhole (referred to as PT signals).[15,16] PT signals from single cells in a linear mode (i.e., without notable cell photodamage) represent a standard positive peak associated with rapid (i.e., pico- to nanosecond scale) cell heating and a slower, microsecond scale tail corresponding to cell cooling. PA and PT methods beneficially supplement each other and, in combination, provide a very powerful theranostic tool. For example, noninvasive PA diagnostics can be combined with PT purging of CTCs and CBCs using more powerful laser pulses.

Labeling in Vivo. A unique advantage of *in vivo* PAFC/PTFC is the possibility for cell detection without labeling, for example by using the positive and negative PA and PT contrast of RBCs and WBCs vs the negative and positive fluorescent contrast of the same cells.[30,42] PA or PT signals can be generated from intrinsic chromophores and pigments such as hemoglobin, melanin, cytochromes, or carotenoids. Also cells with a low endogenous absorption can be labeled directly in the bloodstream through intravenous injection of strongly absorbing functionalized NPs.[2,9,11,13] Depending upon the properties of cells and NPs, the *in vivo* labeling procedure using mouse models takes from 10−20 min to 1 h. Labeling specificity is provided through the selection of molecular markers that are highly expressed in targeted cells (e.g., CTCs and CBCs), but almost absent in normal blood and endothelial cells (e.g., folates in CTCs).[13,22] High labeling efficiency is associated with frequent collisions between NPs and abnormal cells (e.g., CTCs) in partly turbulent blood flow. The PA/PT signals from targeted cells with a typical NP number, for example ranging from 500 to 5000 NPs per CTC cell, are much higher than the PA/PT signal background from RBCs, unbound NPs with typical numbers of 1−10 in the detected volume, or NPs nonspecifically bound to normal blood cells. NP clustering around naturally densely packed cell markers would lead to a significant linear (5−50-fold) and nonlinear (100−300-fold) nanobubble-based enhancement in PA/PT signal amplitude and a red-shift effect in the absorption of coupled NPs in clusters,[16] both of which serve as indicators of successful cell targeting.

Detection Threshold. Two types of NPs were used to estimate the detection threshold sensitivity of PAFC *ex vivo*, including GNTs[12] and magnetic NPs (MNPs).[13] GNTs consist of hollow shortened CNTs surrounded by thin gold layers, averaging 11 nm × 98 nm in diameter and length, respectively. They exhibit high water solubility and biocompatibility, low cytotoxicity (due to the protective layer of gold), and spectrally tunable high plasmon absorption in the NIR range of 700−1000 nm. The minimal number of NPs in the detected (i.e., irradiated) volume that produced readable PA signals in the background of mouse blood in the 120 μm microscopic slide was estimated to be 120 ± 14 for MNPs at 639 nm, and 7 ± 2 for GNTs at 900 nm under laser fluence of 100 mJ/cm^2 in nonlinear mode at both wavelengths, and 35

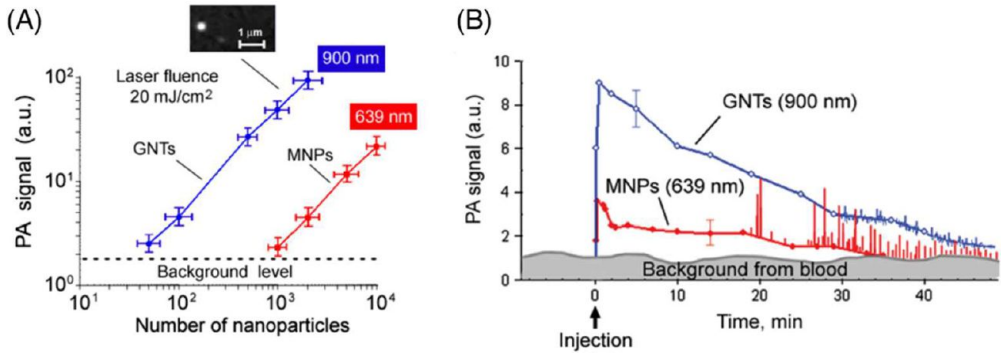

Figure 3. Optimization of NP parameters *in vitro* and *in vivo*. (A) *In vitro* PA signals from NPs at different concentrations in a slide. Callout represents fluorescent images of individual GNTs conjugated with FITC and Abs specific to CD44. (B) *In vivo* measurements of NPs and cells mimicking CTCs. Kinetics of clearance of 30 nm MNPs (red curve with filled circles) and GNTs (blue curve with open circles) at a concentration of 1×10^{11} NPs/mL in a 70 μm mouse ear vein. The error bars represent standard error ($n = 3$). Adapted with permission from ref 13. Copyright 2009 Nature Publishing Group.

for GNTs and 600 for MNPs at laser fluence of 20 mJ/cm^2 (Figure 3A).[13]

The detection threshold sensitivity of PAFC *in vivo* was estimated as follows using GNTs.[12] The 10 μL GNT suspension ($\sim 10^{11}$/mL) was injected intravenously into mice with total blood volume of ~2 mL. Assuming ideal conditions with no loss of GNTs during injection and in circulation, the average GNT concentration in the blood pool should have been 5×10^8 GNTs/mL. The irradiated (detected) volume in blood vessel of mouse ear was limited by laser beam size and the diameter of the vessels. Assuming a linear beam shape with a width of 15 μm and a vessel diameter of 60 μm in mouse ear, the detected volume was estimated as 4.2×10^{-8} cm^3. These parameters correspond to the estimated maximum number of GNTs (around 21) in the detected volume. Taking into account the threshold sensitivity as 7 GNTs at laser fluence 100 mJ/cm^2, it is expected that the signal-to-noise ratio (SNR) *in vivo* in blood vessel is ~3 (i.e., 21/7). However, it was experimentally determined that the SNR is ~7. This discrepancy can be explained by uncontrollable formation of small GNT aggregates in flow, which provided a stronger PA signal as compared to suspensions of single GNTs. Injection of high concentrations of each unconjugated NP alone (iv, $\sim 10^{11}$ NPs/50 μL) in mice revealed their fast clearance during 15–20 min, with no PA detection at low concentrations ($\sim 10^9$ NPs/50 μL) (Figure 3B).

Blood samples collected from mice with tumors at week 1 after cell labeling were put onto a slide with thickness of 120 μm and scanned at a fixed position of focused laser beam (10 μm in diameter). The rare CTCs in blood samples were detected through a remarkable increase in PA signal amplitudes. The presence of cancer cells in a thin blood sample were further verified with optical imaging using specific morphological features such as observing a size greater than normal blood cells. Comparison of PA data *in vivo* and *in vitro* revealed that the threshold sensitivity of PAFC *in vivo* can be estimated as ~1 CTC/mL.[11,32] This threshold sensitivity was primarily limited by the small blood volume (2 mL) in mice rather than PAFC parameters. In humans, sensitivity should be higher by examining large blood volumes circulating through the peripheral vasculature. According to modeling, there is potential to achieve sensitivity of 1 CTC/10 mL (i.e., one order better than existing assays) by monitoring 200–300 μm vessel over ~1 h and to achieve a sensitivity of 1 CTC/100 mL by examining 1–2 mm peripheral blood vessels.

***In Vivo* PAFC/PTFC Nanotheranostic Applications.** *In Vivo Label-Free Theranostics of Melanoma CTCs.* Melanin, which is an intrinsic PA/PT contrast agent, is located in melanoma cells and in ~0.7 μm melanosomes as aggregates of melanin NPs with typical size range of 50–150 nm. Hence, melanoma is an optimal target for PAFC that can facilitate routine, label-free, *in vivo* clinical assessment of CTCs for earlier detection of this most aggressive cancer with increasing incidence rates. In our study, the overexpression of melanin was used as an intrinsic high contrast PA/PT NIR agent, which provided PA signals above the blood absorption background. Real-time PA counting of metastatic melanoma CTCs (B16F10) was performed in a 50 μm diameter vessel in the ear of tumor-bearing mice.[32] CTCs could be readily detected with PAFC weeks before any evidence of detectable metastasis appears in the tissue samples with conventional techniques. The PAFC's sensitivity threshold was found around 1 CTC/mL. This unprecedented threshold sensitivity on the animal model provides an opportunity to use PAFC as a powerful research tool to study CTC behaviors and their role in the development of metastasis at an early cancer stage. As mentioned previously, the PAFC sensitivity has potential to be further improved 100-fold (i.e., ~1 CTC/100 mL), which is unachievable with existing techniques. Also, we recently developed a portable clinical prototype of PAFC using a high-pulse-repetition rate laser at 1064 nm with pulse rates up to 0.5 MHz, fiber delivery of laser radiation, and a focused, ultrasound transducer gently attached to the skin near selected blood vessels.

Increasing the laser energy fluence from 60 mJ/cm^2 to 600 J/cm^2 at 820 nm wavelength, PA contrast of the CTCs increased ~6 times above the RBC background.[32] This effect was associated with laser-induced nanobubbles around over-heated strongly absorbing melanin nanoclusters in melanoma cells, which served as a nonlinear PA signal amplifier compared to linear PA signals from RBCs with homogeneous hemoglobin distribution (i.e., with no nanobubble formation). Also, the rates of CTCs have been gradually decreased from 12 CTC/min to 1–2 CTC/min over a 1 h monitoring period (Figure 4), demonstrating effective purging of circulating melanoma cells. This was also related to the generation of nanobubbles, which served as melanoma cell killers.[15] Further

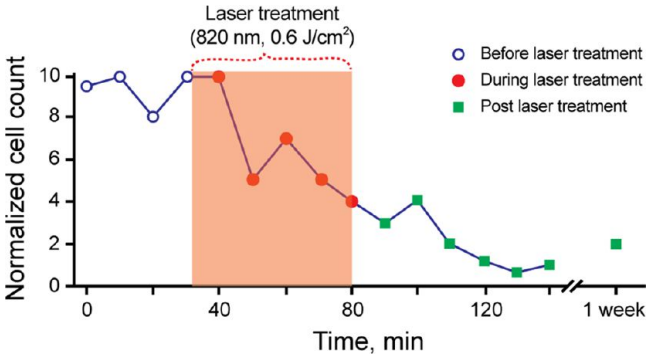

Figure 4. PA guidance of PT therapy of melanoma CTCs. Adapted with permission from ref 11. Copyright 2012 Elsevier.

study could determine whether these new PA/PT theranostics are effective enough to be used alone, or whether it should be used in combination with other therapies such as chemotherapy or radiation therapy.

In Vivo Multiplex, Multicolor, and Multimodal Nanotheranostics of CTCs and CCSCs. To overcome the limits of *ex vivo* detection methods (i.e., small blood sample volume) and increase specificity of *in vivo* CTC detection, we demonstrated, for the first time, the application of magnetic enrichment of CTCs directly in the bloodstream in combination with duplex targeting dual color detection strategy (Figure 5).[13] Highly NIR responsive GNTs (Figure 5C) with an absorption maximum at 900 nm and a minimum at 639 nm (Figure 6D) were coated with polyethylene glycol (PEG) and conjugated with folates. As the second NPs, 10 nm MNPs coated with PEG and amphiphilic triblock polymers were conjugated with the amino-terminal fragment (ATF) of the urokinase plasminogen activator (uPA) (Figure 5B). MNPs have an absorption in a broad NIR range; however, the absorption spectrum is different from that of GNTs (Figure 5D). Injection of cancer cells (iv, 10^5) previously labeled *in vitro* with conjugated MNPs revealed readable PA signals from mimic CTCs with ~40 to 60 min clearance. Using two-color (639 nm/900 nm) PAFC, cell injection alone followed by iv injection of NP cocktail (20:80 conjugated GNT:conjugated MNP) revealed effective labeling within ~5 min after NP injection. The detectable PA signals from CTCs that were double-labeled *in vivo* had clearance rates similar to cells labeled *in vitro*.[13] To detect CTCs originating from a primary tumor, MDA-MB-231 cells were inoculated subcuta-

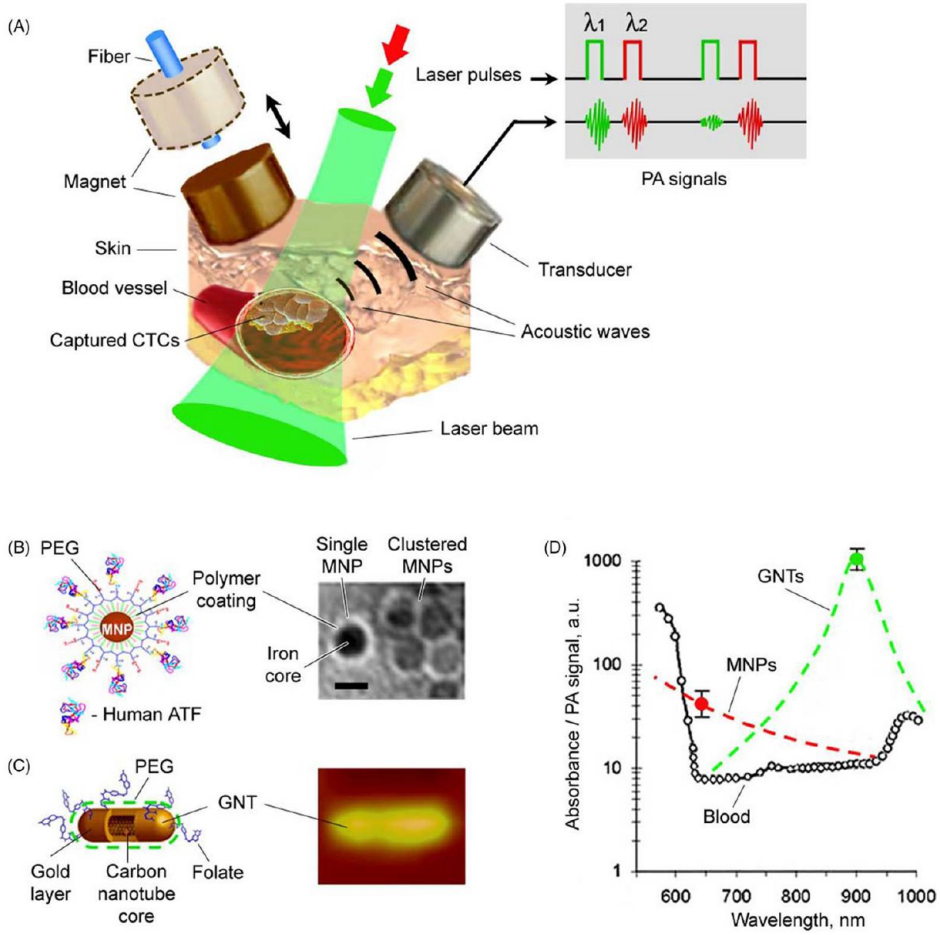

Figure 5. *In vivo* magnetic enrichment and two-color PA detection of CTCs. (A) Schematic with laser beam outside magnet or fiber-based laser delivery through the hole in magnet (dashed lines). (B) The 10 nm MNPs coated with amphiphilic triblock polymers, polyethylene glycol (PEG), and the amino-terminal fragment (ATF). (C) The 12 × 98 nm GNTs coated with PEG and folate. (D) PA spectra of ~70 μm veins in mouse ear (open circles). The average standard deviation for each wavelength is 18%. Absorption spectra of the MNPs and GNTs (dashed curves) normalized to PA signals from CTC labeled with MNPs (red circle) and GNTs (green circle). Adapted with permission from ref 13. Copyright 2009 Nature Publishing Group.

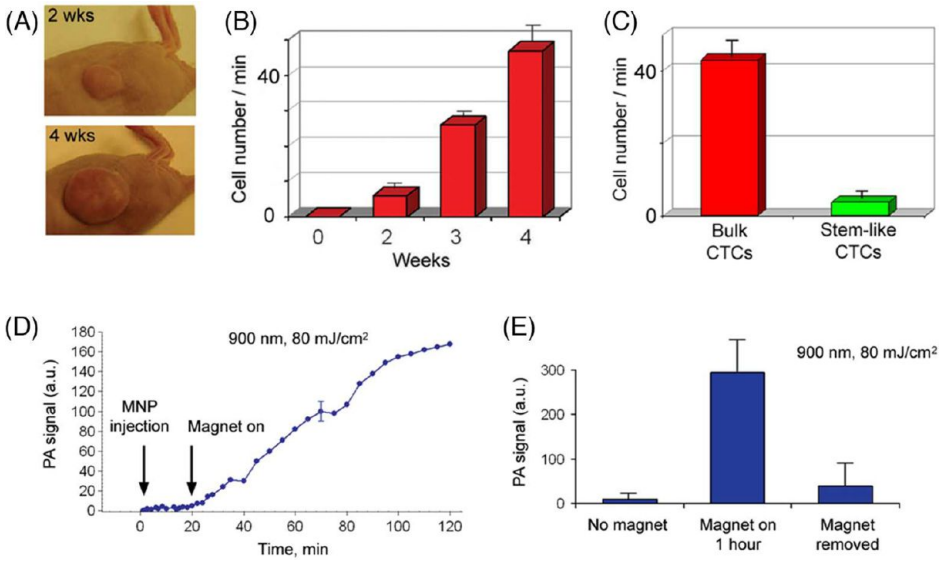

Figure 6. PA detection and magnetic enrichment of CTCs in tumor-bearing mice. (A) The size of the primary breast cancer xenografts at different stages of tumor development. (B) The average rate of CTCs in 200 μm abdominal skin vein over a period of several weeks. (C) Average rate of bulk CTCs and stemlike CTCs in the abdominal skin blood vessels at week 4 of tumor development. (D) PA signals from CTCs in abdominal skin vessels obtained with fiber schematics at week 1 of tumor development before and after magnet action. The average standard deviation for each wavelength is 24%. (E) PA signals from CTCs in abdominal skin vessels before, during (3 min), and after magnetic action at week 2 of tumor development. The error bars in B, C, and E represent standard error (n = 3). Figures were adapted with permission from (A, C) ref 15, copyright 2009 Wiley; (B, D, E) ref 13, copyright 2009 Nature Publishing Group.

neously into nude mice. At 2, 3, and 4 weeks of tumor development (Figure 6A), a cocktail of the conjugated nanoparticles (GNT-folate + MNP-ATF) was injected intravenously into the circulation. Two-color PA detection of CTCs at 20 min after injection (to allow clearance of most unbound nanoparticles) showed that the ratio of the numbers of CTCs in mouse ear to those in abdominal vessels (CTCs per min) increased from (0.9 ± 0.3)/(6 ± 2.1) at 2 weeks to (15.1 ± 2.7)/(47 ± 6.4) at 4 weeks (Figure 6B). These data approximately correlated with the stage of the primary tumor progression. Attaching a magnet with a field strength of 0.39 T at week 1 led to immediate increases in both PA signal amplitude and rate, and changed the character of the PA signal from infrequent flashes to a continuous increase of permanent PA signals up to 88-fold within 1.5 h (Figure 6D,E), indicating successful magnetic CTC capturing.[13] Applying this method to clinical use, patients may potentially carry a magnet attached to selected peripheral vessels (e.g., in the wrist area) for trapping of CTCs, followed by a quick PA detection of the trapped CTCs, and, if necessary, local PT treatment or removal of CTCs by using syringe-based systems for further molecular analysis.

Furthermore, *in vivo* targeting and purging of breast CTCs with a stemlike phenotype (i.e., CCSCs), which are naturally shed from the parent tumor, were performed with two color and dual modal strategy using functionalized GNTs and MNPs.[15] GNTs and MNPs conjugated with folic acid and antibodies to CD44 were selected for the detection of bulk and stemlike CTCs. For identification of bulk CTCs, we used markers described above. At week 4 after tumor inoculation (Figure 6A, bottom), when metastatic lesions developed in the distant organs (e.g., liver), GNT-folate and GNT-CD44 were separately injected iv through mouse tail vein at concentrations of 10^9/mL in 100 μL of PBS (n = 3). PA monitoring of blood vessels began at 20 min after injection to allow effective labeling of CTCs in bloodstream.[11,13] The average rate of flashing PA signals, which is equivalent to the cell rate (i.e., one PA signal corresponds to one cell or cell cluster crossing laser beam) after introduction of GNT-folate, was 42.9 ± 6.5 cells/min. After subsequent injection of GNT-CD44, the rate of flashing PA signals increased to 46.7 ± 6.8 cells/min (Figure 6C). This means that 3.8 ± 0.6 cells/min or 8.8% of all detectable CTCs can be exclusively associated with stemlike subpopulation of CTCs. This study represents the first demonstration of the potential of the multifunctional PAFC/PTFC nanotheranostic platform for ultrasensitive PA molecular detection of CCSCs *in vivo*. Additional studies are needed to develop a fully validated platform. Ongoing studies in our laboratory include exploring the role of the folate receptor and adding CD24 and CD45 markers to increase detection and specificity of CCSCs and exclude possible false positive signals from leukocytes.

In Vivo Multicolor and Multimodal Nanotheranostics of Infected Blood. Bacterial infections are a significant cause of morbidity and mortality worldwide. In particular, multidrug resistant pathogens in the bloodstream are increasingly prevalent problems that complicate the care of many patients. The critical steps in the development of bacterial infections include their penetration into the blood system, interactions with blood cells flowing in the circulatory system or with endothelial cells, and further translocations in the host organisms. Little is known about CBC kinetics in the blood. This includes their clearance and adherence rates, which might be very important for understanding the transition from the bacteremic stage to the tissue invasive stage and for development of an effective therapy. Previously, we demonstrated the capability of the PAFC/PTFC platform to detect and kill, *in vitro*, *Staphylococcus aureus* and *Escherichia coli* labeled with gold NPs and carbon nanotubes (CNTs).[35,38,39] Recently, we extended this platform to include *in vivo*

magnetic enrichment, multiplex PA detection, and PT eradication of circulating *S. aureus* on the basis of the *in vivo* nanotheranostic platform developed for CTCs.[2,13] Bacteria were targeted directly in the bloodstream through intravenous injection of silica-coated MNPs (siMNP) and GNRs functionalized with antibodies specific for *S. aureus* protein A and lipoproteins, respectively. Both antibodies are highly expressed in *S. aureus* and absent in mammalian cells. GNRs had a maximum absorption near 820 nm. After successful two-color PA detection of targeted CBCs at low energy fluence (50 mJ/cm^2) of lasers at 671 and 820 nm, mice were subjected to PT therapy by 1 h laser exposure of a 300 μm abdominal blood vessel with a laser fluence of 0.8 J/cm^2 at 820 nm, coinciding with an absorption spectrum of GNRs. PT nanotherapy led to a significant decrease in the PA signal rate (Figure 7, red curve) compared to the control group (Figure 7, blue curve) at a laser fluence shown to be safe for blood cells. To confirm this therapeutic effect, mice were euthanized, and the blood was examined for the presence of viable bacteria. Blood from mice in the control and PA diagnostic groups showed similar bacterial growth, while the number of bacteria from the PT therapeutic group was reduced by 10-fold. This study implied that the PAFC/PTFC nanotheranostic technical platform may offer unique advantages compared to existing diagnostic and therapeutic approaches: (1) ultrahigh sensitivity (0.5 CFU/mL); (2) physical, PT-based destruction of bacteria, thus retaining its therapeutic efficacy irrespective of antibiotic resistance; (3) integration of multiplex PA molecular detection and PT targeted elimination of CBCs with real-time PA monitoring of therapeutic efficacy; and (4) high spectral specificity based on distinct spectral properties of NPs.[2] Also, the PAFC/PTFC platform has high promise for nanotheranostics of circulating parasites, such as malaria parasites, and other infected cells.

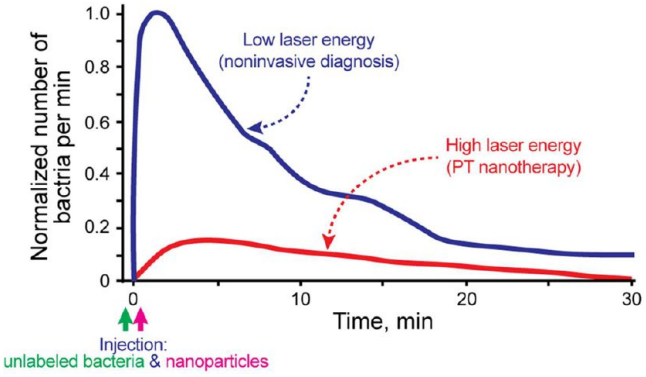

Figure 7. PA molecular diagnosis and PT targeted eradication of circulating *S. aureus* in the blood of the mouse model with real-time PA monitoring of PT nanotherapeutic efficacy. Adapted with permission from ref 2. Copyright 2012 Galanzha et al.

In Vivo Dynamic Interrelations of Blood and Lymph CTCs in Preclinical Studies. Blood and lymph vessels are common pathways for cell dissemination from one location to another through numerous anatomical interconnections between lymph vessels, lymph nodes, and blood circulatory system.[41] The close interrelations of blood and lymph systems can be illustrated by a simplified schematic of dissemination of CTCs in cancer (Figure 8). Logically, to understand disease progression, both lymph and blood pathways should be examined simultaneously. Nevertheless, until now, cells (e.g., CTCs) in blood and lymph have been studied separately, with a particular focus on the role of blood cells. This skewed perspective cannot provide a comprehensive understanding of the mechanisms of disease development. As a result, we currently do not have the clinical capability to intervene and stop development of many diseases at early stage when well-timed treatment is most effective.

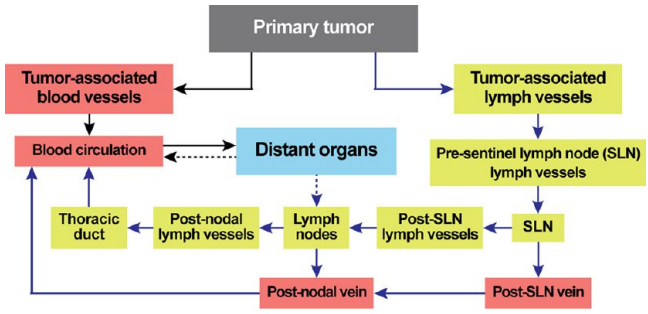

Figure 8. Pathways of CTCs from primary tumor to metastatic sites.

Recently, we integrated blood and lymph PAFC and demonstrated its application in combination with PA lymphography and PA cytometry of sentinel lymph node(s) (SLN; potentially first metastatic site). This platform provided real-time quantitative monitoring of blood and lymph CTCs *in vivo* and defined *in vivo* cross-correlations between lymph CTCs, blood CTCs, size of primary tumor and SLN and distant metastases.[41] The unprecedented sensitivity and specificity allows for the study of CTC pathways at the earliest possible stages of metastatic disease. Specifically, in a preclinical mouse melanoma model, we found that early metastatic cells in latent metastatic disease (1 week after tumor inoculation) can disseminate equally by blood and lymph pathways (Table 1). However, in a few cases, metastatic cells appeared in lymph vessels in week 1 without any cells detected in the blood vessels and vice versa. On average, over the course of two weeks, an increase in the size of a primary tumor by ~3.5 times is associated with an increase in the quantity of lymphatic CTCs by ~10 times, with only a small increase in blood CTCs. The number of PA signals (i.e., number of micrometastases and/or clusters of metastatic cells)[14] from the SLNs increased by 6.5-fold. These data showed that PAFC could clarify dynamic interrelationships of blood and lymph CTCs *in vivo* and their impact on metastasis development.

In Vivo Nanotheranostics of Circulating Blood Clots and Other Applications. When a blood vessel is injured, the normal physiological response of the body is clot (thrombus) formation to prevent blood loss. Alternatively, in the absence of vessel injury, a pathological condition called thromboembolism may lead to formation of circulating blood clots that can block vessels at distant locations, in particular, in peripheral veins (venous thromboembolism), lungs (pulmonary embolism), brain (embolic stroke), heart (myocardial infarction), kidney, or gastrointestinal tract. Thromboembolism is a significant cause of morbidity and mortality, especially in adults. However, little progress has been made in the development of methods for real-time detection and identification of circulating clots. Most emboli are not detected until a vessel obstruction manifests as a serious clinical event.

Commonly used *ex vivo* methods of detecting clots are time-consuming, suffer from poor sensitivity due to the small volumes of blood samples, and are limited by discrete time-

Table 1. Correlation between Primary Tumor Size, Metastasis in SLN, and Number of Tumor Cells in Lymph and Blood Flow of Melanoma-Bearing Mice

		rate of CTCs (cell/min)			
	tumor size (mm^2)	lymph	CTCs	no. of PA signals associated with metastasis in SLNs	histology
1 week	1.0 ± 0.2	0.26 ± 0.05	0.85 ± 0.03	493	no
2 weeks	3.6 ± 0.5	2.13 ± 0.30	1.07 ± 0.05	3188	yes

point sampling with difficult access to clinically relevant sites. Most *in vivo* methods are only able to detect fixed or slowly moving large clots. Pulse Doppler ultrasound is a promising technique for the detection of circulating clots, but this technique cannot detect small clots or assess clot composition and may be affected by artifacts. To overcome these limitations, we proposed an *in vivo* PAFC for real-time detection of clots of different compositions[42,43] using a combination of positive and negative contrast modes. Laser irradiation of blood vessels in normal vessels creates a constant PA background determined by the absorption of RBCs randomly distributed in the irradiated volume. Depending on the size of vessels, hematocrit (Ht), and PAFC spatial resolution, the number of RBCs in the detected volume can vary from one or a few RBCs in a capillary to thousands in larger vessels. When a RBC-rich red clot passes through the irradiated blood volume, a transient increase in the local absorption, which is associated with a high concentration of hemoglobin (Hb), results in a sharp positive PA peak. Red clots can be detected when they have a higher local absorption than the normal RBC background in the detected volume. When a weakly absorbing, platelet rich white clot passes through the laser-irradiated vessel volume, a transient decrease in the local absorption results in a sharp negative PA signal. A mixed clot with both RBC-rich (i.e., high-absorbing) and platelet-rich (i.e., low-absorbing) local zones produces a pattern of positive and negative PA signals.

This phenomenological model was demonstrated in preclinical studies using the mouse model of myocardial infarction created by total ligation of left coronary artery.[42] The readable transient PA signals were observed with different patterns of negative, positive, and combined contrasts associated with white, red, and mixed clots, respectively, compared to no signals in normal control mice. The concentration and size of clots were measured with a threshold of a few clots with diameter of >20 μm in the entire circulation (i.e., 1−3 clots/mL in mice). This PAFC-based diagnostic platform can be used in real time defining risk factors for cardiovascular diseases, as well as for prognosis and potential prevention of stroke by using a well-timed therapy or for a clot count as a marker of therapy efficacy. Besides label-free negative contrast PA detection of clots, they can be potentially targeted by NPs (as CTCs and CBCs) and then destroyed by laser irradiation.

Moreover, NPs with enhanced PA/PT contrast properties were integrated with ultrasound contrast agent (i.e., 0.5−2 μm microbubbles) to enhance the treatment of emboli. Microbubbles were prepared according to standard manufacturer's procedure with modifications by adding absorbing NPs, i.e., CNTs, in various concentrations. PA/PT signals from microbubbles with absorbing agents were significantly higher (10−50-fold) compared to signals from microbubbles or NPs alone. In particular, for intact microbubbles, the threshold for laser-induced evaporation at 850 nm was in the range of 2−8 J/cm^2, while the presence of CNTs reduced this threshold to 10−30 mJ/cm^2 compared to 100−200 mJ/cm^2 for CNTs in water at the similar concentration. Gradual increase of laser energy above evaporation threshold led to sudden nonlinear (10−30-fold) amplification of both PA and PT signals compared to NP solution alone, accompanied by microbubble degradation at high laser energy. After intravenous injection of 100 μL of microbubble solution in the concentration range of 10^{10}−10^{11}/mL to the mouse circulatory system, PAFC revealed quick appearance of many microbubbles with typical clearance of 3−6 min. In the developed model of mouse thrombosis, thrombi with microbubbles could be visualized *in vivo* in blood vessels. Laser irradiation of microbubbles and thrombi *in vitro* and *in vivo* using safe-for-human doses (e.g., 50−100 mJ/cm^2 at 1064 nm) led to the disappearance of both microbubbles and thrombi, suggesting effective destruction and clearance of thrombi.

Finally, we introduced a novel concept of a nanodrug, whose mechanism is based on synergy between physical and biological effects that are photothermally activated in NP−drug conjugates.[44] To prove this concept, we utilized tumor necrosis factor-alpha coated gold nanospheres (Au−TNF) heated by nanosecond laser pulses. To enhance PT nanodrug efficiency in the NIR window of tissue transparency, where nanospheres have off-resonance weak plasmonic absorption, we explored slightly ellipsoidal nanospheres and the occurrence of nanosphere clustering in tumor tissues providing red-shift in plasmonic resonances. In addition, laser−induced dynamic nanoparticle modification and nanobubble formation led to amplification and spectral sharpening of the red-shifted PT resonances. Using a murine carcinoma model, we demonstrated higher PT therapeutic efficacy of Au−TNF conjugates compared to laser and Au−TNF alone or laser with TNF-free gold nanospheres. The PT activation of low toxicity Au−TNF conjugates, which are in phase II trials in humans, with a laser approved for medical applications opens new avenues in the development of clinically relevant PT nanodrugs with synergistic antitumor action.

IN VIVO NANOTHERANOSTICS: TECHNICAL CHALLENGES

The technical challenges facing *in vivo* nanotheranostic platforms fall into one of three categories: (1) the development of suitable contrast nanoagents; (2) the identification of specific and sensitive biomarkers of abnormal circulating features; and (3) the selection of appropriate theranostic modalities. Each category is discussed in detail below.

Development of Novel Contrast Nanoagents. Currently, various nanoscale materials with different shapes, sizes, and compositions are available owing to recent advances in nanotechnology (Figure 9). Unique optical, magnetic, or electronic properties enable their application as imaging and therapeutic contrast agents in different theranostic modalities, including optical, PA, PT, X-ray, positron emission computed tomography (PET), computed tomography (CT), magnetic resonance imaging (MRI), ultrasound (US), etc. Particularly,

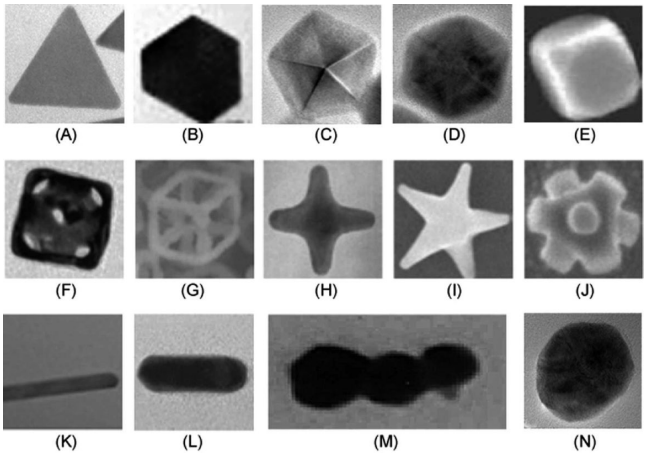

Figure 9. Examples of plasmonic NPs with different shapes. (A) 2D triangle.[115] (B) 2D truncated triangle.[115] (C) 3D decahedron.[115] (D) Hexagonal bipyramidal polygon.[115] (E) Cube.[116] (F) Nanocage.[117] (G) Nanoskeleton.[118] (H) Tetrapod.[119] (I) Star shape.[120] (J) Octapod.[121] (K) Nanobelt.[115] (L) Nanorod.[122] (M) Rod-shape GNT.[12] (N) Spherical colloid.[115] Figures were adapted with permission from (A–D, K, N) ref 115, copyright 2010 Royal Society of Chemistry; (E, F, M) refs 116,117,12 respectively, copyright 2007, 2009, 2009 respectively Nature Publishing Group; (G, I) refs 118,120 respectively, copyright 2009, 2008 respectively Wiley; (H, J, K) refs 119,121,122 respectively, copyright 2008, 2002, 2008 respectively American Chemical Society.

inorganic NPs of different shapes and compositions, including GNSs, GNRs, and GNTs that were tuned to desired NIR spectral ranges, have been reported, and their potential for biomedical imaging and therapy has been demonstrated.[9,12,13,16,21] However, there still is much room to improve the realization of NP-based multicolor, multiplex theranostics. Recent studies indicate that the NIR-responsive NPs have broad plasmonic bands, limiting their multicolor capacity.[13,45,46] There exists great demand for tunable plasmonic nanomaterials with narrow plasmonic bands and distinctive plasmonic signatures especially for optical imaging. With finely tuned plasmonic spectra, multispectral, multicolor, multiplex sensing and imaging is possible. Particularly, the optical tunability and responsiveness in the NIR range (i.e., ~650 to ~1,400 nm) offer promising potential for minimally invasive theranostics of diseases, including tumors and bacterial infections.[2,9,12–16,21,35,38] Most biological components are relatively transparent to NIR. Also NIR responsive NPs allow selective and sensitive sensing of targets in the presence of biological background materials, minimizing the sample preparation and purification time.

Other limitations of many currently available NPs are physicochemical instability, e.g., poor dispersibility in biologically relevant solutions and concerns over NPs' potential toxicity, opsonization, and bioaccumulation, which are major obstacles in translation of NPs to clinical practice. Effective targeting of the intended cells and tissues, especially diseased ones such as tumors and infections, through systemic administration of NPs or their complexes is a major challenge. NPs for nanomedicine-related theranostics typically have low clearance rates from the body and accumulate in the liver and the spleen due to their relatively large sizes (i.e., >30 nm). Recent studies showed that NPs with hydrodynamic diameters less than 5.5 nm are rapidly and efficiently excreted.[47] However, in general, such small NPs are not suitable as imaging contrast agents due to their low responsiveness and poor sensitivity. Thus, there is a need for clever approaches to overcome these limitations. Lastly, for multiplex, quantitative targeting and therapy of circulating tumor cells and biomolecules, NP surfaces should be highly addressable, allowing for the functionalization of different biomarkers, such as antibodies, small RNAs, hormones, or aptamers.

Identification of Specific Markers of Abnormal Cells. The identification of new biomarkers or biomarker signatures that provide both high specificity and high sensitivity for detecting abnormal circulating cells such as CTCs, CBCs, or clots in whole blood is critical to the success of *in vivo* nanotheranostics. Fortunately, bacterial specific markers, such as *S. Aureus* protein A, are well characterized and are not expressed on mammalian cells. In the case of clots, differences in size and absorbance can be used to distinguish normal cells from blood clots.[42] CTCs, on the other hand, are highly heterogeneous, and many CTC biomarkers are also found on normal tissues. As such, the remainder of this section focuses on challenges associated with identifying appropriate CTC markers.

As mentioned previously, our group has explored combinations of folate-conjugated and anti-CD44-conjugated GNTs as well as MNPs conjugated with ATF of uPA to detect CTCs in preclinical models.[13,14] The folate receptor is a promising biomarker as it is highly expressed in 90% of ovarian and endometrial cancers as well as a significant percentage of lung, kidney, breast, and uterine cancers.[48–50] In normal tissues with the exception of kidney, folate receptors are found on luminal surfaces of epithelial tissues and thus are shielded from the circulation.[49,51] Low et al. have demonstrated that intravital multiphoton microscopy can detect CTCs in tumor bearing mice injected with fluorescence-labeled folate.[22] Advantages of folate over tumor-specific antibodies for labeling CTCs include (1) the small size of folate (MW = 441), which allows for rapid clearance ($t_{1/2}$ = 3–5 min)[22] thus reducing the opportunity for nonspecific binding; and (2) the high density of folate receptors on some tumor cells allowing for more intense labeling than antibodies.[52] Key limitations of folate targeting are that (1) folate receptor expression is cancer- and patient-specific; and (2) folate receptors can be shed into the blood and circulate unattached from CTCs.[53,54]

CD44 is a receptor for hyaluronic acid. It is a commonly used marker to help identify CCSCs,[55] however, CD44 is ubiquitously expressed on both hematopoietic and non-hematopoietic cells. For this reason, additional markers such as CD24 and CD133 are also used in CCSC detection. While the use of multiple markers is expected to increase specificity, sensitivity will decrease.

uPA is a serine protease that regulates matrix degradation, cell invasion, and angiogenesis. The receptor for uPA (uPAR) is highly expressed in 54 to 90% of breast cancers and 86% of pancreatic cancers as well as many other cancer types.[56,57] uPAR is expressed at low levels in normal tissues, however, it is highly expressed on leukocytes during infection, on various tissues in various inflammatory disorders, and in wound response, which may lead to high background levels.[58] Another challenge posed by uPAR is that it can be secreted into the circulation and thus interfere with binding of nanotheranostics to CTCs.

Because of the limited number of studies focusing on *in vivo* CTC detection, it is useful to review some of the cell surface

biomarkers used by the various *in vitro* CTC detection schemes. The same or related markers can be adapted for *in vivo* CTC detection.

Epithelial Markers. Cancers of epithelial origin account for approximately 80% of all cancer diagnoses. It follows that epithelial markers have become the most common class of markers for CTC detection *in vitro*. EpCAM (CD326) is expressed by the majority of epithelial cancers and is not believed to be expressed by leukocytes or erythrocytes. However, a subset of B cells has been found to bind EpCAM-specific antibodies.[59] Fortunately, the use of lineage specific markers, such as CD45, can be used to exclude leukocytes. Antibodies are susceptible to nonspecific binding by Fc receptors that are expressed by monocytes and granulocytes. EpCAM-specific antibodies are used to label and enrich CTCs in the CellSearch and other *ex vivo/in vitro* assays. Interpatient and intrapatient variability of EpCAM expression is a major limitation. Comprehensive analyses of EpCAM expression in primary tumors demonstrate a high level of variability. For example, 32% of bladder cancers, 32−42% of ductal carcinomas, 41% of squamous cell carcinomas of the cervix, vagina, and vulva, 71% of hormone refractory prostate cancers, 73% of ovarian cancers, 78% of pancreatic adenocarcinomas, and 81% of colon adenocarcinomas were positive for EpCAM.[60,61]

Cytokeratins (CKs), intermediate cytoskeletal filaments found in the cytoplasm of epithelial cells, are another epithelium marker frequently used to identify CTCs. In particular, expression of CK 8, CD 18, and/or CK 19 has been linked with various epithelial cancers. CK expression is highly variable and less specific than EpCAM expression. In fact, the percentage of CK positive cells in healthy individuals ranges from 0% to 20%.[62,63] Furthermore, because CKs are primarily located in the cytoplasm, CTC detection using CKs requires cell permeabilization and fixation that are impractical for *in vivo* studies. Current CTC detection methods that utilize EpCAM for enrichment and CK markers for identification fail to detect CTCs in 43−80% of patients with metastatic disease.[64]

Disadvantages of using epithelial markers to detect CTCs are 3-fold. First and foremost, epithelial-mesenchymal transition (EMT) is cited as a likely, if not common, mechanism of metastasis.[1,65] Cells undergoing EMT down-regulate epithelial markers such as EpCAM and CK while upregulating mesenchymal markers such as vimentin, N-cadherin, and fibronectin. In fact, micrometastatic deposits isolated from the bone marrow of breast cancer patients were found to completely lose epithelial CK expression in favor of vimentin. Cells that have lost epithelial characteristics in favor of a more invasive mesenchymal phenotype are thought to have a better chance of surviving in circulation and extravasating to form a metastatic lesion. These cells which have a higher metastatic potential are excluded by CTC detection methods considering only epithelial markers.[66]

Second, epithelial cells that lose cell-to-cell contact typically undergo apoptosis: a process called anoikis. As such, the vast majority of epithelial CTCs may be destined for apoptosis and clearance. This assumption seems to agree with Fidler's estimate that only about 0.01% of CTCs result in a metastatic lesion. Since each gram of tumor sheds about 1×10^6 cells into the circulation per day,[67,68] detection of CTCs by epithelial markers may be better suited to assess overall tumor burden than metastatic potential.

The third disadvantage of epithelial markers is that peripheral blood is routinely contaminated with normal epithelial cells that have entered the circulation due to tissue trauma, noncancerous inflammation, or iatrogenic procedures.[6,69] The use of epithelial markers alone, therefore, may overestimate the prevalence of CTCs.

Tumor-Associated Markers. Human Epidermal Growth Factor Receptor 2 (HER2) is a biomarker for breast cancer where it is overexpressed in approximately 30% of patients and associated with a more aggressive phenotype. HER2 is also overexpressed in ovarian, uterine, and gastrointestinal malignancies. While HER2 has been used to detect CTCs, several studies have shown differences in HER2 expression between a primary tumor and CTCs. Specifically, $HER2^-$ CTCs have been found in patients with $HER2^+$ breast cancer[70] and $HER2^+$ CTC in patients with $HER2^-$ primary tumors.[71−73]

While prostate specific antigen (PSA) is the standard biomarker for prostate cancer, anti-PSA antibodies have been found to bind to monocytes.[63] Fortunately, prostate specific membrane antigen (PSMA) has proven to be a more useful marker for the detection of CTCs *in vitro*.[74]

Carcinoembryonic antigen (CEA) and mucin 1 (MUC1) are glycoproteins that are overexpressed in a wide range of malignancies. Both CEA[75,76] and MUC1[77] have been used to detect CTCs in cancer patients. The shedding of both glycoproteins into the circulation complicates their use for *in vivo* detection.

Stem Cell Markers. Regardless of whether or not CCSCs are truly "stem" cells or simply more aggressive, tumor initiating cells, the identification of this population is important for both cancer prognosis and treatment. A number of studies have isolated cancer stem or stemlike cells from clinical samples. A single definitive marker for cancer stem cells has yet to be identified for any cancer type. As such, recent studies have focused on the discovery of rare subsets expressing multiple markers. Human breast carcinoma cells that were $CD44^+CD24^{-/low}$ $Lineage^-$ exhibited enhanced tumorigenicity consistent with a stemlike cancer cell.[25] $CD44^-CD24^-CD326^+$ cells were recently identified as a novel subpopulation of pancreatic cancer tumor initiating cells.[78] $CD133^+$ colon adenocarcinoma cells were found to be responsible for tumor initiation,[79] whereas $CD44^+CD24^-CD133^+$ breast cancer cells were found to be highly tumorigenic and drug resistant.[80]

Mesenchymal Markers. EMT is cited as a likely, if not common, mechanism of metastasis. As mentioned previously, epithelial markers, e.g., EpCAM, CK, and E-cadherin, are downregulated during EMT while mesenchymal markers, e.g., N-cadherin, vimentin, and fibronectin, are upregulated. However, relatively few studies have investigated mesenchymal markers on the surfaces of CTCs compared to the wealth of studies using epithelial markers. A recent study has identified a subset of CTCs expressing a mesenchymal phenotype, i.e., $vimentin^+$ $N\text{-}cadherin^+$, in patients with squamous cell carcinoma of the head and neck.[81] In lung cancer patients, vimentin was expressed on a fraction of CTCs but the majority of cells in circulating tumor microemboli (CTM).[82] CTM are multicellular aggregates of tumor cells that likely have survival and proliferative advantages in establishing metastases.[82,83]

Endothelial Markers. There are also known progenitor cells of the endothelial lineage circulating to different extents in

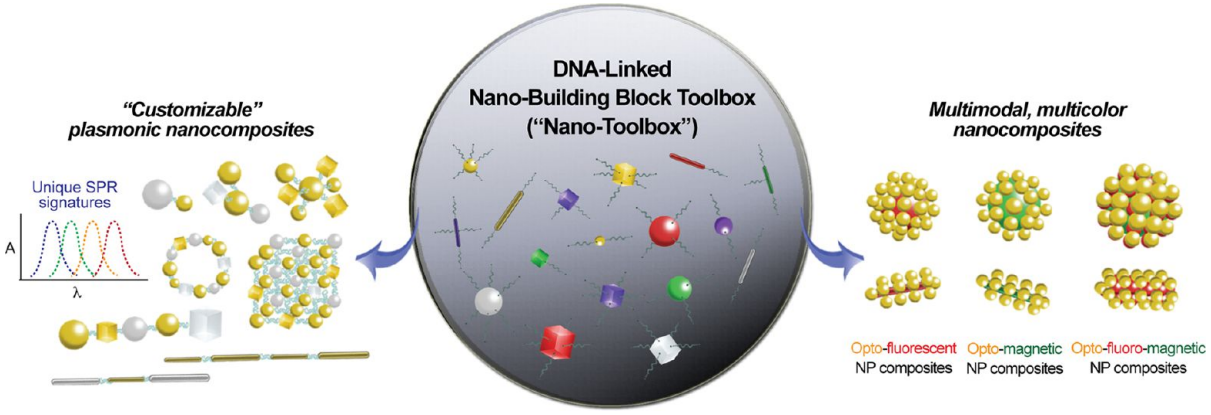

Figure 10. Schematic of a nano-building block toolbox (nanotoolbox) for programmable self-assembly of multifunctional nanostructures with arbitrary shapes and functions, and examples of applications of self-assembled multifunctional nanocomposites with shapes, sizes, and functions that are "programmable/customizable" on the basis of the target applications.[98] Customizable plasmonic nanomaterials with distinct plasmonic signatures using metallic NP building blocks of various sizes and shapes (left). Multimodal, multicolor contrasting nanoagents through controlled integration of heterogeneous multiple discrete NP building blocks with various sizes and shapes into single multifunctional nanoscale architectures with predefined characteristics (right). The nanocomposite's surface is addressable, allowing for the multiplex functionalization of different biomolecules, including antibodies, small RNAs, aptamers, hormones, etc. Figures were adapted with permission from refs 98,104, copyright 2012 and 2011 respectively Wiley.

normal and cancer-bearing patients. There has been an increasing implication of progenitor cell contribution to neovascularization processes in the body, including tumor growth.[84−90] Further evidence has suggested that endostatin or other inhibitors of angiogenesis perturbs mobilization of these cells.[89,91−93] We have been investigating the proangiogenic activity and radiation biology of circulating endothelial progenitors using blood outgrowth endothelial cells (BOEC). BOEC, which are endothelial cell precursors, are isolated from human peripheral blood and grown in culture. After multifold expansion these cells express several endothelial protein markers: VE Cadherin (VEC), von Willebrand factor (vWF), PECAM (CD31), and P1H12.[87] Our preliminary results show that injection of these cells can augment the rate of tumor growth, improve tumor oxygenation, and modify radiation response (manuscript in submission). This indicates that existing endothelial progenitors in the circulation may be a significant factor in tumor vascularization, growth, environment, and treatment response. These novel discoveries point to the possibility that progenitor cells are a target for antiangiogenesis strategies and are involved in the response of tissue to treatment related damage (radiation or chemotherapy).[94] Therefore, attempts to determine the degree to which theranostic nanomedicine approaches can control or inhibit populations of circulating endothelial cells are warranted.

Selection of Appropriate Theranostic Modalities. MRI, PET, CT, US, X-ray, Raman scattering, fluorescence optical imaging, and laser-induced PA and PT imaging are among the theranostic modalities available in the clinic. The selection of the proper modality for accurate and reliable diagnostic imaging is a considerable task that clinicians confront. Each modality has pros and cons in terms of sensitivity, spatial and temporal resolution, and imaging depth.[95−98] For example, modalities with high sensitivity, such as optical imaging and PET, have comparatively inadequate resolution; however, those with high resolution, such as CT and MRI, possess relatively low sensitivity. The integration of multiple imaging modalities has gained interest to realize more accurate and reliable diagnostics. Although there are clear merits of combining multiple modalities in tandem, they should be selected rationally through careful considerations of characteristics of each modality, so that they may compensate for the deficits of each individual modality to maximize their synergistic effects.[96] One such example would be the integration of PET or optical imaging with high sensitivity with MRI or CT with high spatial resolution. Furthermore, most of the modalities require exogenic contrast agents to improve the signal-to-noise ratio. The amount of different contrast agents required for multiple modalities with different resolutions and sensitivities can be a problem. Nanoagents that contain multiple functionalities, such as optical plasmon resonance, photoluminescence, magnetism, etc., would offer distinct advantages.[96−98] Such multifunctional nanoagents could be detected by multiple imaging modalities, significantly improving their performance in theranostics and facilitating the early detection of tumors. Also the use of a single contrast agent warrants consistent and reproducible pharmacokinetics and targeting specificity for each diagnostic modality. Moreover, the single multimodal probe could reduce the problems related to sequestration in the liver as well as toxicity issues by minimizing the total amount of contrast agent administered for the multiple imaging modalities.[96,98] Despite the promises, the controlled synthesis of rationally designed multifunctional contrast nanoagents remains very challenging.

■ STRATEGIES AND FUTURE PERSPECTIVES

Here we outline strategies to overcome existing challenges and facilitate further development of *in vivo* nanotheranostics. A vision for future clinical application of these technologies is also presented.

Multifunctional Theranostic Contrast Nanoagents. There has been considerable interest in development of multifunctional nanocomposites with defined shapes and sizes that incorporate diverse nanocomponents.[95−98] The use of various types of NPs with unique physicobiochemical properties would enable us to develop multimodal nanoagents, with which multiple tasks and functionalities could be performed sequentially or simultaneously.[98] This strategy

would allow us to obtain more comprehensive, accurate, and reliable information by coupling the complementary abilities of different imaging and therapeutic modalities.

The assembly of these nanocomposites can be driven by DNA, owing to its unique molecular recognition properties, structural features, and ease of manipulation, In fact, DNA-driven self-assembly has demonstrated the potential to program matter at a molecular scale for the generation of new material properties.[98−101] Like DNA, RNA could self-assemble to synthesize various nanostructures that could assemble into NPs with desirable functionalities.[102,103] However, the accurate, scalable, and high-rate assembly of heterogeneous nanocomponents into multifunctional nanostructures with specifically designed shapes and sizes remains difficult to achieve.

The site-specific functionalization of multiple strands of DNA or RNA to the NP surface in a well-defined and stoichiometric manner is a prerequisite to control the spatial arrangement of NPs in the nanostructures.[98] NP building blocks with control over DNA or RNA number and geometric configuration on their surface would realize enhanced control over the shape and function of final self-assembled structures. Recently, Kim et al.[104,105] reported a novel anisotropic monofunctionalization strategy to place different number of DNA linkers on a NP at specific angles to each other and to synthesize NP building blocks with well-defined arrangements of DNA in all three dimensions (Figure 10).[98,104] Also this technology could incorporate NPs of different composition. Such well-defined and controlled functionality and directionality of various NP building blocks promise precisely controlled manufacture of structures with greater complexity for "customized" size, shape, and functionality. Engineering the sizes and structural configurations of nanocomposites offers exciting possibility to customize plasmonic nanomaterials (Figure 10).[98] Geometric factors, such as shape and size, and material compositions influence the optical properties, such as extinction and scattering spectra, of nanomaterials.[98] Hence, the self-organization of metallic NPs of various sizes and shapes into desired patterns and geometries could realize enhanced optical response over several wavelength bands. With multiple nanocomposites of finely tuned plasmonic spectra, multispectral, multicolor imaging is possible. In addition, the length of the DNA linkers could control the spacing between NPs, leading to dramatic increases in the sensitivity by controlling the plasmonic interactions between adjacent NPs.[98] This would realize highly selective and sensitive theranostics by matching the nanocomposites' plasmonic spectra and resonant laser wavelengths. Furthermore, the controlled integration of various types of NPs would open another significant possibility of multimodal theranostics. Combining the useful functionalities of different NPs in a single nanostructure would allow new multiple complementary imaging modes for faster, more efficient, more accurate prognosis. Nonetheless, to realize such promising applications, we should be able to control the interactions among NPs with different functionalities, such as electronic, magnetic, and optical. With the DNA-programmable building blocks of different NPs, the NP spacing could be accurately tuned by modulating the DNA lengths to minimize their negative interactions, such as the long-standing problems of the fluorescence quenching of fluorophores and quantum dots by metallic NP surface,[106,107] promote enhanced new properties, and achieve desired multifunctionalities. The functionality of self-assembled nanocomposites can also be tuned by controlling their shape and size as well as thickness of each NP layer. Moreover, the nanocomposite's surface is addressable. DNA sequences on the outer layer of the nanocomposite can serve as specific anchor points for incorporating multiple biorecognition units. This enables highly selective and controllable attachment of various recognition units, such as antibodies, small RNAs, hormones, and aptamers, allowing multiplex quantitative targeting and therapy to be possible. The successful merger of desirable functionalities of various NPs in a controlled manner should enable us to realize highly sensitive, multiplex, multicolor nanotheranostics for circulating tumor cells and pathological biomolecules with multiple complementary modalities beyond the inherent limitations of individual existing technologies.[98] Of note is that RNA could provide similar attributes of DNA in the nanostructure self-assembly with a distinctive advantage. RNA could be designed and manipulated with a similar level of simplicity as DNA to produce a variety of different nanostructures. RNA possess catalytic functions similar to proteins and their nanostructures, such as small interfering RNA (siRNA), microRNA (miRNA), RNA aptamers and ribozymes, demonstrating promise for theranostics of cancers and infections.[102] Hence, the polyvalent nature of RNA nanostructures and their incorporation in the NP-building block technology not only could provide a new tool for the theranostics of metastatic cells but also could lead to developing noble strategies for *in vivo* multifunctional nanotheranostics.

In addition, Zharov et al. recently discovered ultrasharp PA/PT resonances in plasmonic NPs with a spectral width down to 0.8 nm (i.e., 100-fold narrower than linear absorption spectra).[44,45] This would offer another promising way to overcome the challenges related to the relatively broad absorption bands of PA/PT contrast agents (e.g., 60−150 nm for GNRs or GNSs), which limit their multicolor capacity (i.e., restrict them to only two simultaneous colors).[9,13,45,46] The physical mechanism underlying these phenomena is based on multistage signal behaviors as energy fluence (E) increases: (1) a linear increase at low fluence, E^n ($n \approx 1$), (2) strong nonlinear nanobubble-associated 10−100-fold signal amplification ($n \approx 2$−5), (3) signal saturation ($n \approx 0$−0.5), and (4) further enhanced or inhibited signal depending on NP type. Thus, a shift of the laser wavelength toward the absorption center leads to increased energy absorption, raising the temperature above the well-defined nanobubble-formation threshold and accompanied by a significant (10−100-fold) signal amplification. As a result, spectrally dependent signal amplification led to the sharpening of PT resonances only near the centers of absorption peaks. Higher laser energy above the nanobubble threshold nonlinear spectral resonances can be red-shifted from the linear absorption spectra. This approach made it possible to easily identify each GNR in a mixture of 7 GNRs with nearly overlapping longitudinal plasmon resonances, which were hardly distinguishable by conventional absorption spectra. Thus, up to 6−8 multicolor functionalized NPs whose nonlinear spectra do not overlap in the window of tissue transparency (650−1,100 nm) can be used to simultaneously target 6−8, and potentially more, biomarkers.

Furthermore, self-assembled nanocomposites could alleviate concerns regarding bioaccumulation and potential toxicity of NPs. The NP building blocks could be very small, on the order of ∼3 nm.[104] The assembly is driven by DNA, a

biodegradable biopolymer. When structures are together, the self-assembled nanocomposites can be large enough to be effective theranostic contrast nanoagents; however, the structural building blocks are small enough to be effectively cleared from the body when disassembled by, for example, DNA denaturation through localized laser-induced heating or eventual nuclease-driven DNA digestion/biodegradation.[98]

Also, the addressable nanocomposite surface could offer ways to avoid clearance to the liver and spleen by macrophages after intravenous injection. The fates of foreign NPs and their composites in blood depend upon their physicochemical properties, including size, shape, and surface chemistry.[108,109] Modulating the geometric configurations and surface characteristics suggests opportunities to overcome the hurdle and considerably prolong blood circulation times, which is particularly important for effective theranostics of circulating tumor-associated cells and biomolecules. Biocompatible and opsonin resistant moieties, such as biological and chemical ligands like dextran sulfate and polyethylene glycol,[110−112] can be site-specifically attached to the self-assembled nanocomposite surface to shield them from opsonization and ensure their prolonged circulation. In addition, there exist many biological particles, such as blood cells and pathogenic bacteria, that have evolved to evade opsonins. Using lessons from nature, the design and construction of nanocomposites with particular shapes and surface characteristics may permit us to similarly avoid opsonization and premature clearance of nanotheranostics.[98] Taken together, the ability to engineer nanocomposites through self-assembly with DNA-linked NP building blocks promises to enable realization of *in vivo* nanotheranostic platforms with multicolor and multimodal capability and their translation into clinical practice.

CTC Markers and the Biology of Metastasis. The success of *in vivo* CTC nanotheranostics will hinge upon the specificity of CTC markers. Given the heterogeneous expression of CTC markers in different types and stages of cancer as well as inter- and intrapatient variability, it is clear that a single CTC marker or even a single class of markers will be insufficient to provide a complete account of CTCs. Furthermore, current *in vivo* and *in vitro* CTC detection technologies are susceptible to high false-positive rates due to nonspecific binding and high false-negative rates due to loss of marker expression.

Multimodal *in vivo* nanotheranostics can be developed to overcome these challenges by developing a set of CTC markers that can be imaged simultaneously. For example, folate, anti-vimentin, anti-CD44, anti-EpCAM and anti-CEA can be conjugated to unique contrast agents (e.g., self-assembled multifunctional nanocomposites) and imaged at different wavelengths. Such an approach would provide more information about the heterogeneity of CTCs and may help identify CTC subsets with higher metastatic potential.

Fidler's estimate that only 0.01% of CTCs result in a metastatic lesion[28] indicates that the vast majority of CTCs have no role in metastasis. A key question to be addressed is whether the 0.01% represents a unique phenotype. It has been postulated that metastasis is a rare event because it demands a cell endowed with many capabilities: a "decathlon champion".[29] One expects such a cell to have a unique phenotype and that the standard $EpCAM^+CK^+$ signature of a CTC will not fit. The use of different classes of markers, e.g., tumor-associated, mesenchymal, stem cell etc., would be better suited for the detection of a "decathlete" cell.

Multifunctional *in vivo* nanotheranostics will also allow us to study rare CTC subsets in greater detail. For example, MNPs can be used to capture CTCs *in vivo*[13] prior to extraction via minimally invasive surgery or fine-needle aspiration. Extracted CTCs can then be characterized *in vitro* through gene expression analyses or functional assays.

Opportunity for Synergy with Targeted Therapeutics Delivery. The programmable self-assembly of nanocomposites with DNA- or RNA-NP building blocks may offer a clever way to achieve highly targeted drug delivery that maximizes therapeutic efficacy while minimizing side effects. The NP nanostructure could be designed and assembled to be drug-delivery vesicles, for example, with 3D shapes with hollow cores to carry pharmacologically active agents. These nanovesicles can be programmed to be responsive to specific stimuli for the controlled release of drugs. For instance, if a part of the nanostructure were composed of a particular type of NPs that uniquely responded to a particular resonant laser wavelength yet the other NPs in the rest of the structure did not, localized laser-induced heating could selectively denature DNA linkages and cause a specific release of drug. Also DNA sequences of a specific part of the structure could be designed so that it may open by strand displacement with particular DNA oligonucleotide inputs.[113] This would enable delivery of toxic agents in a highly programmable manner, alleviating the limitations of conventional drug therapy by substantially reducing the drug doses as well as drug toxicity, yet maximizing its therapeutic efficacy. Since these drug carriers are constructed on the basis of the same assembly technology as the aforementioned multifunctional nanocomposites, they should seamlessly integrate into the *in vivo* multimodal nanotheranostic platform.

Recently, we have found that an antiangiogenic peptide (named anginex) increases tumor sensitivity to radiation in animal models due to its antiangiogenic properties by binding to galectin-1 on the cell surface.[114,123] In addition, we observed that anginex treatment iv blunts the angiogenic effects of CECs injected into mice early in tumor growth, resulting in smaller tumors. After introducing exogenous CECs, we have found that tumors consistently grow to larger sizes. When the growth rates of tumors exposed to exogenous CECs were compared to those treated with both CECs and the antiangiogenic peptide, we observed that the antiangiogenic effects are exerted through a pathway that includes blocking at least part of the activity/viability of CECs. *In vitro* studies have shown that peptide alone decreases the number of surviving CEC colonies after a 4 h exposure by about 20%. Importantly, we also noted an increased sensitivity to ionizing radiation in CECs pretreated with the peptide, with a decrease of CEC viability of nearly 90% in the combination treatment group. These results suggest that targeting the CECs with a peptide conjugated to a nanoprobe may allow efficient targeting and destruction by our *in vivo* PAFC and PTFC strategies. In addition, we may be able to sensitize these CECs or other malignant cells to other therapies by administering multifunctional nanoprobes, such as NP nanoarchitectures "customized" with desired size, shape and functionality using our "enabling" DNA-programmable NP building block technology.

CONCLUSION

Early detection increases the probability of successful treatment of all diseases: from cancers to cardiovascular disorders to bacterial infections. Recent technological advances have sparked interest in the early detection of harbingers of disease, such as CTCs, CECs, CCSCs, CBCs and circulating blood clots, in the cardiovascular and lymphatic circulations. As outlined in this review, *in vivo* nanotheranostic platforms have a number of key advantages in this regard. *In vivo* detection techniques allow for interrogation of the entire blood volume of the patient, thus increasing the probability of detecting rare events. The use of nanotheranostics *in vivo* also permits continuous monitoring of physiology. Lastly, the development of multifunctional contrast nanoagents provides opportunities for simultaneous detection and purging of circulating features via multiple modalities. In particular, substantial progress has been made with *in vivo* real-time PAFC/PTFC nanotheranostics. These platforms are capable of integrating magnetic enrichment, multispectral PA detection and PT therapy with a potential for multiplex targeting of diverse biomarkers. These platforms are also clinically relevant given that (1) low toxicity NPs are used as contrast agents and (2) diagnostic lasers for PAFC/PTFC not only are used at safe fluence levels but also penetrate deeply in biological tissues.

Despite recent progress, several challenges must be overcome before *in vivo* nanotheranostics reach their full clinical potential. Continued exploration of contrast nanoagents must find spectrally distinct NPs that avoid opsonization and liver/spleen accumulation. Unique complexes of NPs, e.g., "customizable" NP nanocomposites self-assembled by our programmable DNA/RNA-NP building block toolbox technology, which respond to multiple modalities as well as deliver therapeutic agents or local hyperthermia, are a particularly fertile area of exploration. Separately, more specific biomarkers are needed to overcome high background noise in highly complex whole blood as well as inter- and intrapatient heterogeneity. Finally, the appropriate selection or development of multiple imaging modalities must coincide with multifunctional features of contrast nanoagents.

If these challenges are met, the presented innovative PA and PT technological platforms with "programmable/customizable" multifunctional nanoagents may catalyze a paradigm shift in medicine from the treatment of symptomatic disease to the application of therapeutic interventions before symptoms appear to preserve normal function and decrease morbidity.

AUTHOR INFORMATION

Corresponding Author

*J.-W.K.: Tel: +1-479-575-2351. Fax: +1-479-575-2846. E-mail: jwkim@uark.edu. V.P.Z.: E-mail: ZharovVladimirP@umas.edu.

Notes

The authors declare no competing financial interest.

ACKNOWLEDGMENTS

This work was supported in part by National Science Foundation grants (CMMI 1235100, ECCS 1137948 and 11228660, and DBI 0852737), National Institutes of Health grants (R01EB000873, R01CA131164, R01EB009230, R01CA44114, R21CA139373 and K22CA131567), Department of Defense grants (W88XWH-10-2-0130, W81XWH-11-1-0123 and W81XWH-11-1-0129), and the Arkansas Biosciences Institute. The authors thank Min Kim and Jeong-Min Lim for their assistance in image processing.

REFERENCES

(1) Chaffer, C. L.; Weinberg, R. A. A perspective on cancer cell metastasis. *Science* **2011**, *331*, 1559−64.

(2) Galanzha, E. I.; Shashkov, E.; Sarimollaoglu, M.; Beenken, K. E.; Basnakian, A. G.; Shirtliff, M. E.; Kim, J.-W.; Smeltzer, M. S.; Zharov, V. P. *In vivo* magnetic enrichment, photoacoustic diagnosis, and photothermal purging of infected blood using multifunctional gold and magnetic nanoparticles. *PLoS One* **2012**, *7*, e45557.

(3) Pantel, K.; Alix-Panabieres, C. Circulating tumour cells in cancer patients: challenges and perspectives. *Trends Mol. Med.* **2010**, *16*, 398−406.

(4) Yu, M.; Stott, S.; Toner, M.; Maheswaran, S.; Haber, D. A. Circulating tumor cells: approaches to isolation and characterization. *J. Cell Biol.* **2011**, *192*, 373−82.

(5) Alix-Panabieres, C.; Schwarzenbach, H.; Pantel, K. Circulating tumor cells and circulating tumor DNA. *Annu. Rev. Med.* **2012**, *63*, 199−215.

(6) Paterlini-Brechot, P.; Benali, N. L. Circulating tumor cells (CTC) detection: clinical impact and future directions. *Cancer Lett.* **2007**, *253*, 180−204.

(7) Maheswaran, S.; Haber, D. A. Circulating tumor cells: a window into cancer biology and metastasis. *Curr. Opin. Genet. Dev.* **2010**, *20*, 96−9.

(8) Zhe, X.; Cher, M. L.; Bonfil, R. D. Circulating tumor cells: finding the needle in the haystack. *Am. J. Cancer Res.* **2011**, *1*, 740−51.

(9) de la Zerda, A.; Kim, J.-W.; Galanzha, E. I.; Gambhir, S. S.; Zharov, V. P. Advanced contrast nanoagents for photoacoustic molecular imaging, cytometry, blood test and photothermal theranostics. *Contrast Media Mol. Imaging* **2011**, *6*, 346−69.

(10) Hughes, A. D.; King, M. R. Nanobiotechnology for the capture and manipulation of circulating tumor cells. *WIREs Nanomed. Nanobiotechnol.* **2012**, *4*, 291−309.

(11) Galanzha, E. I.; Zharov, V. P. Photoacoustic flow cytometry. *Methods* **2012**, *57*, 280−96.

(12) Kim, J.-W.; Galanzha, E. I.; Shashkov, E. V.; Moon, H.-M.; Zharov, V. P. Golden carbon nanotubes as multimodal photoacoustic and photothermal high-contrast molecular agents. *Nat. Nanotechnol.* **2009**, *4*, 688−94.

(13) Galanzha, E. I.; Shashkov, E. V.; Kelly, T.; Kim, J.-W.; Yang, L.; Zharov, V. P. *In vivo* magnetic enrichment and multiplex photoacoustic detection of circulating tumour cells. *Nat. Nanotechnol.* **2009**, *4*, 855−60.

(14) Galanzha, E. I.; Kokoska, M. S.; Shashkov, E. V.; Kim, J.-W.; Tuchin, V. V.; Zharov, V. P. *In vivo* fiber-based multicolor photoacoustic detection and photothermal purging of metastasis in sentinel lymph nodes targeted by nanoparticles. *J. Biophotonics* **2009**, *2*, 528−39.

(15) Galanzha, E. I.; Kim, J.-W.; Zharov, V. P. Nanotechnology-based molecular photoacoustic and photothermal flow cytometry platform for in-vivo detection and killing of circulating cancer stem cells. *J. Biophotonics* **2009**, *2*, 725−35.

(16) Zharov, V. P.; Kim, J.-W.; Curiel, D. T.; Everts, M. Self-assembling nanoclusters in living systems: application for integrated photothermal nanodiagnostics and nanotherapy. *Nanomedicine* **2005**, *1*, 326−45.

(17) Nie, S.; Xing, Y.; Kim, G. J.; Simons, J. W. Nanotechnology applications in cancer. *Annu. Rev. Biomed. Eng.* **2007**, *9*, 257−88.

(18) De, M.; Ghosh, P. S.; Rotello, V. M. Applications of Nanoparticles in Biology. *Adv. Mater.* **2008**, *20*, 4225−41.

(19) Lee, S. E.; Lee, L. P. Biomolecular plasmonics for quantitative biology and nanomedicine. *Curr. Opin. Biotechnol.* **2010**, *21*, 489−97.

(20) Giljohann, D. A.; Seferos, D. S.; Daniel, W. L.; Massich, M. D.; Patel, P. C.; Mirkin, C. A. Gold nanoparticles for biology and medicine. *Angew. Chem., Int. Ed.* **2010**, *49*, 3280−94.
(21) Lal, S.; Clare, S. E.; Halas, N. J. Nanoshell-enabled photothermal cancer therapy: impending clinical impact. *Acc. Chem. Res.* **2008**, *41*, 1842−51.
(22) He, W.; Wang, H.; Hartmann, L. C.; Cheng, J. X.; Low, P. S. *In vivo* quantitation of rare circulating tumor cells by multiphoton intravital flow cytometry. *Proc. Natl. Acad. Sci. U.S.A.* **2007**, *104*, 11760−5.
(23) Georgakoudi, I.; Solban, N.; Novak, J.; Rice, W. L.; Wei, X.; Hasan, T.; Lin, C. P. In vivo flow cytometry: a new method for enumerating circulating cancer cells. *Cancer Res.* **2004**, *64*, 5044−5047.
(24) Bonnet, D.; Dick, J. E. Human acute myeloid leukemia is organized as a hierarchy that originates from a primitive hematopoietic cell. *Nat. Med.* **1997**, *3*, 730−7.
(25) Al-Hajj, M.; Wicha, M. S.; Benito-Hernandez, A.; Morrison, S. J.; Clarke, M. F. Prospective identification of tumorigenic breast cancer cells. *Proc. Natl. Acad. Sci. U.S.A.* **2003**, *100*, 3983−8.
(26) Chiang, A. C.; Massague, J. Molecular basis of metastasis. *N. Engl. J. Med.* **2008**, *359*, 2814−23.
(27) Ailles, L. E.; Weissman, I. L. Cancer stem cells in solid tumors. *Curr. Opin. Biotechnol.* **2007**, *18*, 460−6.
(28) Fidler, I. J. Metastasis: quantitative analysis of distribution and fate of tumor embolilabeled with 125 I-5-iodo-2′-deoxyuridine. *J. Natl. Cancer Inst.* **1970**, *45*, 773−82.
(29) Fidler, I. J. The pathogenesis of cancer metastasis: the 'seed and soil' hypothesis revisited. *Nat. Rev. Cancer* **2003**, *3*, 453−8.
(30) Nedosekin, D. A.; Sarimollaoglu, M.; Galanzha, E. I.; Sawant, R.; Torchilin, V. P.; Verkhusha, V. V.; Ma, J.; Frank, M. H.; Biris, A. S.; Zharov, V. P. Synergy of photoacoustic and fluorescence flow cytometry of circulating cells with negative and positive contrasts. *J. Biophotonics* **2013**, DOI: 10.1002/jbio.201200047(in press).
(31) Zharov, V. P.; Galanzha, E. I.; Tuchin, V. V. Photothermal imaging of moving cells in lymph and blood flow in vivo. *Proc. SPIE* **2004**, *5320*, 185. DOI: 10.1117/12.532107.
(32) Galanzha, E. I.; Shashkov, E. V.; Spring, P. M.; Suen, J. Y.; Zharov, V. P. *In vivo*, noninvasive, label-free detection and eradication of circulating metastatic melanoma cells using two-color photoacoustic flow cytometry with a diode laser. *Cancer Res.* **2009**, *69*, 7926−34.
(33) Nedosekin, D. A.; Sarimollaoglu, M.; Ye, J. H.; Galanzha, E. I.; Zharov, V. P. *In vivo* ultra-fast photoacoustic flow cytometry of circulating human melanoma cells using near-infrared high-pulse rate lasers. *Cytometry, Part A* **2011**, *79*, 825−33.
(34) Sarimollaoglu, M.; Nedosekin, D. A.; Simanovsky, Y.; Galanzha, E. I.; Zharov, V. P. *In vivo* photoacoustic time-of-flight velocity measurement of single cells and nanoparticles. *Opt. Lett.* **2011**, *36*, 4086−8.
(35) Zharov, V. P.; Galanzha, E. I.; Shashkov, E. V.; Kim, J.-W.; Khlebtsov, N. G.; Tuchin, V. V. Photoacoustic flow cytometry: principle and application for real-time detection of circulating single nanoparticles, pathogens, and contrast dyes *in vivo*. *J. Biomed. Opt.* **2007**, *12*, 051503.
(36) Galanzha, E. I.; Shashkov, E. V.; Tuchin, V. V.; Zharov, V. P. In vivo multispectral, multiparameter, photoacoustic lymph flow cytometry with natural cell focusing, label-free detection and multicolor nanoparticle probes. *Cytometry, Part A* **2008**, *73*, 884−94.
(37) Nedosekin, D. A.; Sarimollaoglu, M.; Shashkov, E. V.; Galanzha, E. I.; Zharov, V. P. Ultra-fast photoacoustic flow cytometry with a 0.5 MHz pulse repetition rate nanosecond laser. *Optics Express* **2010**, *18*, 8605−20.
(38) Kim, J.-W.; Shashkov, E. V.; Galanzha, E. I.; Kotagiri, N.; Zharov, V. P. Photothermal antimicrobial nanotherapy and nanodiagnostics with self-assembling carbon nanotube clusters. *Lasers Surg. Med.* **2007**, *39*, 622−34.
(39) Zharov, V. P.; Mercer, K. E.; Galitovskaya, E. N.; Smeltzer, M. S. Photothermal nanotherapeutics and nanodiagnostics for selective killing of bacteria targeted with gold nanoparticles. *Biophys. J.* **2006**, *90*, 619−27.
(40) Zharov, V. P.; Galanzha, E. I.; Shashkov, E. V.; Khlebtsov, N. G.; Tuchin, V. V. In vivo photoacoustic flow cytometry for monitoring of circulating single cancer cells and contrast agents. *Opt. Lett.* **2006**, *31*, 3623−25.
(41) Galanzha, E. I. Blood and lymph circulating cells: well-known systems, well-forgotten interdependence. *J. Blood Lymph* **2011**, *1*, 1−2.
(42) Galanzha, E. I.; Sarimollaoglu, M.; Nedosekin, D. A.; Keyrouz, S. G.; Mehta, J. L.; Zharov, V. P. *In vivo* flow cytometry of circulating clots using negative photothermal and photoacoustic contrasts. *Cytometry, Part A* **2011**, *79*, 814−24.
(43) Galanzha, E. I.; Zharov, V. P. *In vivo* photoacoustic and photothermal cytometry for monitoring multiple blood rheology parameters. *Cytometry, Part A* **2011**, *79*, 746−57.
(44) Shao, J.; Griffin, R. J.; Galanzha, E. I.; Kim, J.-W.; Koonce, N.; Webber, J.; Mustafa, T.; Biris, A.; Nedosekin, D. A.; Zharov, V. P. Photothermal nanodrugs: potential of TNF-fold nanospheres for cancer theranostics. *Sci. Rep.* **2013**, 10.038/srep 01293 (in press).
(45) Zharov, V. P. Ultrasharp nonlinear photothermal and photoacoustic resonances and holes beyond the spectral limit. *Nat. Photonics* **2011**, *5*, 110−6.
(46) Li, P. C.; Wei, C. W.; Liao, C. K.; Chen, C. D.; Pao, K. C.; Wang, C. R.; Wu, Y. N.; Shieh, D. B. Photoacoustic imaging of multiple targets using gold nanorods. *IEEE Trans Ultrason. Ferroelectr. Freq. Control* **2007**, *54*, 1642−7.
(47) Choi, H. S.; Liu, W.; Misra, P.; Tanaka, E.; Zimmer, J. P.; Itty Ipe, B.; Bawendi, M. G.; Frangioni, J. V. Renal clearance of quantum dots. *Nat. Biotechnol.* **2007**, *25*, 1165−70.
(48) Allard, J. E.; Risinger, J. I.; Morrison, C.; Young, G.; Rose, G. S.; Fowler, J.; Berchuck, A.; Maxwell, G. L. Overexpression of folate binding protein is associated with shortened progression-free survival in uterine adenocarcinomas. *Gynecol. Oncol.* **2007**, *107*, 52−7.
(49) Clifton, G. T.; Sears, A. K.; Clive, K. S.; Holmes, J. P.; Mittendorf, E. A.; Ioannides, C. G.; Ponniah, S.; Peoples, G. E. Folate receptor alpha: a storied past and promising future in immunotherapy. *Hum. Vaccines* **2011**, *7*, 183−90.
(50) Hartmann, L. C.; Keeney, G. L.; Lingle, W. L.; Christianson, T. J.; Varghese, B.; Hillman, D.; Oberg, A. L.; Low, P. S. Folate receptor overexpression is associated with poor outcome in breast cancer. *Int. J. Cancer* **2007**, *121*, 938−42.
(51) Sega, E. I.; Low, P. S. Tumor detection using folate receptor-targeted imaging agents. *Cancer Metastasis Rev.* **2008**, *27*, 655−64.
(52) He, W.; Kularatne, S. A.; Kalli, K. R.; Prendergast, F. G.; Amato, R. J.; Klee, G. G.; Hartmann, L. C.; Low, P. S. Quantitation of circulating tumor cells in blood samples from ovarian and prostate cancer patients using tumor-specific fluorescent ligands. *Int. J. Cancer* **2008**, *123*, 1968−73.
(53) Basal, E.; Eghbali-Fatourechi, G. Z.; Kalli, K. R.; Hartmann, L. C.; Goodman, K. M.; Goode, E. L.; Kamen, B. A.; Low, P. S.; Knutson, K. L. Functional folate receptor alpha is elevated in the blood of ovarian cancer patients. *PLoS One* **2009**, *4*, e6292.
(54) Kamen, B. A.; Caston, J. D. Direct radiochemical assay for serum folate: competition between 3H-folic acid and 5-methyltetrahydrofolic acid for a folate binder. *J. Lab. Clin. Med.* **1974**, *83*, 164−74.
(55) Woodward, W. A.; Sulman, E. P. Cancer stem cells: markers or biomarkers? *Cancer Metastasis Rev.* **2008**, *27*, 459−70.
(56) Yang, L.; Mao, H.; Cao, Z.; Wang, Y. A.; Peng, X.; Wang, X.; Sajja, H. K.; Wang, L.; Duan, H.; Ni, C.; Staley, C. A.; Wood, W. C.; Gao, X.; Nie, S. Molecular imaging of pancreatic cancer in an animal model using targeted multifunctional nanoparticles. *Gastroenterology* **2009**, *136*, 1514−25.e2.
(57) Yang, L.; Peng, X. H.; Wang, Y. A.; Wang, X.; Cao, Z.; Ni, C.; Karna, P.; Zhang, X.; Wood, W. C.; Gao, X.; Nie, S.; Mao, H. Receptor-targeted nanoparticles for *in vivo* imaging of breast cancer. *Clin. Cancer Res.* **2009**, *15*, 4722−32.

(58) Blasi, F.; Carmeliet, P. uPAR: a versatile signalling orchestrator. *Nat. Rev. Mol. Cell Biol.* **2002**, *3*, 932−43.
(59) Eifler, R. L.; Lind, J.; Falkenhagen, D.; Weber, V.; Fischer, M. B.; Zeillinger, R. Enrichment of circulating tumor cells from a large blood volume using leukapheresis and elutriation: proof of concept. *Cytometry, Part B* **2011**, *80*, 100−11.
(60) Spizzo, G.; Fong, D.; Wurm, M.; Ensinger, C.; Obrist, P.; Hofer, C.; Mazzoleni, G.; Gastl, G.; Went, P. EpCAM expression in primary tumour tissues and metastases: an immunohistochemical analysis. *J. Clin. Pathol.* **2011**, *64*, 415−20.
(61) Went, P. T.; Lugli, A.; Meier, S.; Bundi, M.; Mirlacher, M.; Sauter, G.; Dirnhofer, S. Frequent EpCam protein expression in human carcinomas. *Hum. Pathol.* **2004**, *35*, 122−8.
(62) Fehm, T.; Solomayer, E. F.; Meng, S.; Tucker, T.; Lane, N.; Wang, J.; Gebauer, G. Methods for isolating circulating epithelial cells and criteria for their classification as carcinoma cells. *Cytotherapy* **2005**, *7*, 171−85.
(63) Wang, Z. P.; Eisenberger, M. A.; Carducci, M. A.; Partin, A. W.; Scher, H. I.; Ts'o, P. O. Identification and characterization of circulating prostate carcinoma cells. *Cancer* **2000**, *88*, 2787−95.
(64) Allard, W. J.; Matera, J.; Miller, M. C.; Repollet, M.; Connelly, M. C.; Rao, C.; Tibbe, A. G.; Uhr, J. W.; Terstappen, L. W. Tumor cells circulate in the peripheral blood of all major carcinomas but not in healthy subjects or patients with nonmalignant diseases. *Clin. Cancer Res.* **2004**, *10*, 6897−904.
(65) Mego, M.; Mani, S. A.; Cristofanilli, M. Molecular mechanisms of metastasis in breast cancer—clinical applications. *Nat. Rev. Clin. Oncol.* **2010**, *7*, 693−701.
(66) Gorges, T. M.; Tinhofer, I.; Drosch, M.; Roese, L.; Zollner, T. M.; Krahn, T.; von Ahsen, O. Circulating tumour cells escape from EpCAM-based detection due to epithelial-to-mesenchymal transition. *BMC Cancer* **2012**, *12*, 178.
(67) Butler, T. P.; Gullino, P. M. Quantitation of cell shedding into efferent blood of mammary adenocarcinoma. *Cancer Res.* **1975**, *35*, 512−6.
(68) Liotta, L. A.; Kleinerman, J.; Saidel, G. M. Quantitative relationships of intravascular tumor cells, tumor vessels, and pulmonary metastases following tumor implantation. *Cancer Res.* **1974**, *34*, 997−1004.
(69) Crisan, D.; Ruark, D. S.; Decker, D. A.; Drevon, A. M.; Dicarlo, R. G. Detection of circulating epithelial cells after surgery for benign breast disease. *Mol. Diagn.* **2000**, *5*, 33−8.
(70) Powell, A. A.; Talasaz, A. H.; Zhang, H.; Coram, M. A.; Reddy, A.; Deng, G.; Telli, M. L.; Advani, R. H.; Carlson, R. W.; Mollick, J. A.; Sheth, S.; Kurian, A. W.; Ford, J. M.; Stockdale, F. E.; Quake, S. R.; Pease, R. F.; Mindrinos, M. N.; Bhanot, G.; Dairkee, S. H.; Davis, R. W.; Jeffrey, S. S. Single cell profiling of circulating tumor cells: transcriptional heterogeneity and diversity from breast cancer cell lines. *PLoS One* **2012**, *7*, e33788.
(71) Meng, S.; Tripathy, D.; Frenkel, E. P.; Shete, S.; Naftalis, E. Z.; Huth, J. F.; Beitsch, P. D.; Leitch, M.; Hoover, S.; Euhus, D.; Haley, B.; Morrison, L.; Fleming, T. P.; Herlyn, D.; Terstappen, L. W.; Fehm, T.; Tucker, T. F.; Lane, N.; Wang, J.; Uhr, J. W. Circulating tumor cells in patients with breast cancer dormancy. *Clin. Cancer Res.* **2004**, *10*, 8152−62.
(72) Tewes, M.; Aktas, B.; Welt, A.; Mueller, S.; Hauch, S.; Kimmig, R.; Kasimir-Bauer, S. Molecular profiling and predictive value of circulating tumor cells in patients with metastatic breast cancer: an option for monitoring response to breast cancer related therapies. *Breast Cancer Res Treat.* **2009**, *115*, 581−90.
(73) Wulfing, P.; Borchard, J.; Buerger, H.; Heidl, S.; Zanker, K. S.; Kiesel, L.; Brandt, B. HER2-positive circulating tumor cells indicate poor clinical outcome in stage I to III breast cancer patients. *Clin. Cancer Res.* **2006**, *12*, 1715−20.
(74) Kirby, B. J.; Jodari, M.; Loftus, M. S.; Gakhar, G.; Pratt, E. D.; Chanel-Vos, C.; Gleghorn, J. P.; Santana, S. M.; Liu, H.; Smith, J. P.; Navarro, V. N.; Tagawa, S. T.; Bander, N. H.; Nanus, D. M.; Giannakakou, P. Functional characterization of circulating tumor cells with a prostate-cancer-specific microfluidic device. *PLoS One* **2012**, *7*, e35976.
(75) Iinuma, H.; Watanabe, T.; Mimori, K.; Adachi, M.; Hayashi, N.; Tamura, J.; Matsuda, K.; Fukushima, R.; Okinaga, K.; Sasako, M.; Mori, M. Clinical significance of circulating tumor cells, including cancer stem-like cells, in peripheral blood for recurrence and prognosis in patients with Dukes' stage B and C colorectal cancer. *J. Clin. Oncol.* **2011**, *29*, 1547−55.
(76) Shimada, R.; Iinuma, H.; Akahane, T.; Horiuchi, A.; Watanabe, T. Prognostic significance of CTCs and CSCs of tumor drainage vein blood in Dukes' stage B and C colorectal cancer patients. *Oncol. Rep.* **2012**, *27*, 947−53.
(77) de Cremoux, P.; Extra, J. M.; Denis, M. G.; Pierga, J. Y.; Bourstyn, E.; Nos, C.; Clough, K. B.; Boudou, E.; Martin, E. C.; Muller, A.; Pouillart, P.; Magdelenat, H. Detection of MUC1-expressing mammary carcinoma cells in the peripheral blood of breast cancer patients by real-time polymerase chain reaction. *Clin. Cancer Res.* **2000**, *6*, 3117−22.
(78) Jaiswal, K. R.; Xin, H. W.; Anderson, A.; Wiegand, G.; Kim, B.; Miller, T.; Hari, D.; Ray, S.; Koizumi, T.; Rudloff, U.; Thorgeirsson, S. S.; Avital, I. Comparative testing of various pancreatic cancer stem cells results in a novel class of pancreatic-cancer-initiating cells. *Stem Cell Res.* **2012**, *9*, 249−60.
(79) O'Brien, C. A.; Pollett, A.; Gallinger, S.; Dick, J. E. A human colon cancer cell capable of initiating tumour growth in immunodeficient mice. *Nature* **2007**, *445*, 106−10.
(80) Wright, M. H.; Calcagno, A. M.; Salcido, C. D.; Carlson, M. D.; Ambudkar, S. V.; Varticovski, L. Brca1 breast tumors contain distinct CD44+/CD24- and CD133+ cells with cancer stem cell characteristics. *Breast Cancer Res.* **2008**, *10*, R10.
(81) Balasubramanian, P.; Lang, J. C.; Jatana, K. R.; Miller, B.; Ozer, E.; Old, M.; Schuller, D. E.; Agrawal, A.; Teknos, T. N.; Summers, T. A., Jr.; Lustberg, M. B.; Zborowski, M.; Chalmers, J. J. Multi-parameter Analysis, including EMT Markers, on Negatively Enriched Blood Samples from Patients with Squamous Cell Carcinoma of the Head and Neck. *PLoS One* **2012**, *7*, e42048.
(82) Hou, J. M.; Krebs, M.; Ward, T.; Sloane, R.; Priest, L.; Hughes, A.; Clack, G.; Ranson, M.; Blackhall, F.; Dive, C. Circulating tumor cells as a window on metastasis biology in lung cancer. *Am. J. Pathol.* **2011**, *178*, 989−96.
(83) Christiansen, J. J.; Rajasekaran, A. K. Reassessing epithelial to mesenchymal transition as a prerequisite for carcinoma invasion and metastasis. *Cancer Res.* **2006**, *66*, 8319−26.
(84) Jiang, Y.; Jahagirdar, B. N.; Reinhardt, R. L.; Schwartz, R. E.; Keene, C. D.; Ortiz-Gonzalez, X. R.; Reyes, M.; Lenvik, T.; Lund, T.; Blackstad, M.; Du, J.; Aldrich, S.; Lisberg, A.; Low, W. C.; Largaespada, D. A.; Verfaillie, C. M. Pluripotency of mesenchymal stem cells derived from adult marrow. *Nature* **2002**, *418*, 41−9.
(85) Reyes, M.; Dudek, A.; Jahagirdar, B.; Koodie, L.; Marker, P. H.; Verfaillie, C. M. Origin of endothelial progenitors in human postnatal bone marrow. *J. Clin. Invest.* **2002**, *109*, 337−46.
(86) Kalka, C.; Masuda, H.; Takahashi, T.; Kalka-Moll, W. M.; Silver, M.; Kearney, M.; Li, T.; Isner, J. M.; Asahara, T. Transplantation of ex vivo expanded endothelial progenitor cells for therapeutic neovascularization. *Proc. Natl. Acad. Sci. U.S.A.* **2000**, *97*, 3422−7.
(87) Lin, Y.; Weisdorf, D. J.; Solovey, A.; Hebbel, R. P. Origins of circulating endothelial cells and endothelial outgrowth from blood. *J. Clin. Invest.* **2000**, *105*, 71−7.
(88) Takahashi, T.; Kalka, C.; Masuda, H.; Chen, D.; Silver, M.; Kearney, M.; Magner, M.; Isner, J. M.; Asahara, T. Ischemia- and cytokine-induced mobilization of bone marrow-derived endothelial progenitor cells for neovascularization. *Nat. Med.* **1999**, *5*, 434−8.
(89) Mancuso, P.; Calleri, A.; Cassi, C.; Gobbi, A.; Capillo, M.; Pruneri, G.; Martinelli, G.; Bertolini, F. Circulating endothelial cells as a novel marker of angiogenesis. *Adv. Exp. Med. Biol.* **2003**, *522*, 83−97.
(90) Rehman, J.; Li, J. L.; Orschell, C. M.; March, K. L. Peripheral blood "endothelial progenitor cells" are derived from monocyte/

macrophages and secrete angiogenic growth factors. *Circulation* **2003**, *107*, 1164−9.
(91) Jain, R. K.; Duda, D. G. Role of bone marrow-derived cells in tumor angiogenesis and treatment. *Cancer Cell* **2003**, *3*, 515−6.
(92) Ruzinova, M. B.; Schoer, R. A.; Gerald, W.; Egan, J. E.; Pandolfi, P. P.; Rafii, S.; Manova, K.; Mittal, V.; Benezra, R. Effect of angiogenesis inhibition by Id loss and the contribution of bone-marrow-derived endothelial cells in spontaneous murine tumors. *Cancer Cell* **2003**, *4*, 277−89.
(93) Schuch, G.; Heymach, J. V.; Nomi, M.; Machluf, M.; Force, J.; Atala, A.; Eder, J. P., Jr.; Folkman, J.; Soker, S. Endostatin inhibits the vascular endothelial growth factor-induced mobilization of endothelial progenitor cells. *Cancer Res.* **2003**, *63*, 8345−50.
(94) Brower, V. Evidence of efficacy: researchers investigating markers for angiogenesis inhibitors. *J. Natl. Cancer Inst.* **2003**, *95*, 1425−7.
(95) Nie, Z.; Petukhova, A.; Kumacheva, E. Properties and emerging applications of self-assembled structures made from inorganic nanoparticles. *Nat. Nanotechnol.* **2010**, *5*, 15−25.
(96) Louie, A. Y. Multimodality Imaging Probes: Design and Challenges. *Chem. Rev.* **2010**, *110*, 3146−95.
(97) Jin, Y.; Jia, C.; Huang, S. W.; O'Donnell, M.; Gao, X. Multifunctional nanoparticles as coupled contrast agents. *Nat. Commun.* **2010**, *1*, 41.
(98) Kim, J.-W.; Deaton, R. Molecular self-assembly of multifunctional nanoparticle composites with arbitrary shapes and functions: challenges and strategies. *Part. Part. Syst. Charact.* **2013**, doi: 10.1002/ppsc.201200129 (in press).
(99) Jones, M. R.; Osberg, K. D.; Macfarlane, R. J.; Langille, M. R.; Mirkin, C. A. Templated Techniques for the Synthesis and Assembly of Plasmonic Nanostructures. *Chem. Rev.* **2011**, *111*, 3736−827.
(100) Pinheiro, A. V.; Han, D.; Shih, W. M.; Yan, H. Challenges and opportunities for structural DNA nanotechnology. *Nat. Nanotechnol.* **2011**, *6*, 763−72.
(101) Tan, S. J.; Campolongo, M. J.; Luo, D.; Cheng, W. Building plasmonic nanostructures with DNA. *Nat. Nanotechnol.* **2011**, *6*, 268−76.
(102) Guo, P. X. The emerging field of RNA nanotechnology. *Nat. Nanotechnol.* **2010**, *5*, 833−42.
(103) Shu, D.; Shu, Y.; Haque, F.; Abdelmawla, S.; Guo, P. X. Thermodynamically stable RNA three-way junction for constructing multifunctional nanoparticles for delivery of therapeutics. *Nat. Nanotechnol.* **2011**, *6*, 658−67.
(104) Kim, J.-W.; Kim, J.-H.; Deaton, R. DNA-linked nanoparticle building blocks for programmable matter. *Angew. Chem., Int. Ed.* **2011**, *50*, 9185−90.
(105) Kim, J.-W.; Kim, J.-H.; Deaton, R. Programmable construction of nanostructures: assembly of nanostructures with various nanocomponents. *IEEE Nanotechnol.* **2012**, *6* (1), 19−23.
(106) Dubertret, B.; Calame, M.; Libchaber, A. J. Single-mismatch detection using gold-quenched fluorescent oligonucleotides. *Nat. Biotechnol.* **2001**, *19*, 365−70.
(107) Pons, T.; Medintz, I. L.; Sapsford, K. E.; Higashiya, S.; Grimes, A. F.; English, D. S.; Mattoussi, H. On the quenching of semiconductor quantum dot photoluminescence by proximal gold nanoparticles. *Nano Lett.* **2007**, *7*, 3157−64.
(108) Champion, J. A.; Mitragotri, S. Role of target geometry in phagocytosis. *Proc. Natl. Acad. Sci. U.S.A.* **2006**, *103*, 4930−4.
(109) Alexis, F.; Pridgen, E.; Molnar, L. K.; Farokhzad, O. C. Factors affecting the clearance and biodistribution of polymeric nanoparticles. *Mol. Pharmaceutics* **2008**, *5*, 505−15.
(110) Otsuka, H.; Nagasaki, Y.; Kataoka, K. PEGylated nanoparticles for biological and pharmaceutical applications. *Adv. Drug Delivery Rev.* **2003**, *55*, 403−19.
(111) Kotagiri, N.; Kim, J.-W. Carbon Nanotubes Fed on "Carbs": Coating of Single-Walled Carbon Nanotubes by Dextran Sulfate. *Macromol. Biosci.* **2010**, *10*, 231−8.
(112) Kotagiri, N.; Lee, J. S.; Kim, J.-W. Selective pathogen targeting and macrophage evading carbon nanotubes through dextran sulfate coating and PEGylation for photothermal theranostics. *J. Biomed. Nanotechnol.* **2013**, doi: 10.1166/jbn.2013.1531 (in press).
(113) Andersen, E. S.; Dong, M.; Nielsen, M. M.; Jahn, K.; Subramani, R.; Mamdouh, W.; Golas, M. M.; Sander, B.; Stark, H.; Oliveira, C. L. P.; Pedersen, J. S.; Birkedal, V.; Besenbacher, F.; Gothelf, K. V.; Kjems, J. Self-assembly of a nanoscale DNA box with a controllable lid. *Nature* **2009**, *459*, 73−6.
(114) Dings, R. P. M.; Williams, B. W.; Song, C. W.; Griffioen, A. W.; Mayo, K. H.; Griffin, R. J. Anginex synergizes with radiation therapy to inhibit tumor growth by radiosensitizing endothelial cells. *Int. J. Cancer* **2005**, *115*, 312−9.
(115) Kim, J.-W.; Moon, H.-M.; Benamara, M.; Sakon, J.; Salamo, G. J.; Zharov, V. P. Aqueous-phase synthesis of monodisperse plasmonic gold nanocrystals using shortened single-walled carbon nanotubes. *Chem. Commun.* **2010**, *46*, 7142−4.
(116) Tao, A.; Sinsermsuksakul, P.; Yang, P. Tunable plasmonic lattices of silver nanocrystals. *Nat. Nanotechnol.* **2007**, *2*, 435−40.
(117) Yavuz, M. S.; Cheng, Y. Y.; Chen, J. Y.; Cobley, C. M.; Zhang, Q.; Rycenga, M.; Xie, J. W.; Kim, C.; Song, K. H.; Schwartz, A. G.; Wang, L. H. V.; Xia, Y. N. Gold nanocages covered by smart polymers for controlled release with near-infrared light. *Nat. Mater.* **2009**, *8*, 935−9.
(118) Wang, X.; Fu, H. B.; Peng, A. D.; Zhai, T. Y.; Ma, Y.; Yuan, F. L.; Yao, J. N. One-Pot Solution Synthesis of Cubic Cobalt Nanoskeletons. *Adv. Mater.* **2009**, *21*, (16) doi: 10.1002/adma.200990051.
(119) Seo, D.; Il Yoo, C.; Chung, I. S.; Park, S. M.; Ryu, S.; Song, H. Shape adjustment between multiply twinned and single-crystalline polyhedral gold nanocrystals: Decahedra, icosahedra, and truncated tetrahedra. *J. Phys. Chem. C* **2008**, *112*, 2469−75.
(120) Liao, H. G.; Jiang, Y. X.; Zhou, Z. Y.; Chen, S. P.; Sun, S. G. Shape-Controlled Synthesis of Gold Nanoparticles in Deep Eutectic Solvents for Studies of Structure-Functionality Relationships in Electrocatalysis. *Angew. Chem., Int. Ed.* **2008**, *47*, 9100−3.
(121) Sun, Y. G.; Mayers, B. T.; Xia, Y. N. Template-engaged replacement reaction: A one-step approach to the large-scale synthesis of metal nanostructures with hollow interiors. *Nano Lett.* **2002**, *2*, 481−5.
(122) Ni, W. H.; Yang, Z.; Chen, H. J.; Li, L.; Wang, J. F. Coupling between molecular and plasmonic resonances in freestanding dye-gold nanorod hybrid nanostructures. *J. Am. Chem. Soc.* **2008**, *130*, 6692−3.
(123) Pagan, J.; Przybyla, B.; Jamshidi-Parsian, A.; Gupta, K.; Griffin, R. J. Blood outgrowth endothelial cells increase tumor growth rates and modify tumor physiology: relevance for therapeutic targeting. *Cancers* **2013**, *5*, 205−17.

■ NOTE ADDED AFTER ASAP PUBLICATION

This paper was published on the Web on February 25, 2013. Citations have been corrected in the first two paragraphs of the *IN VIVO* NANOTHERANOSTICS OF CIRCULATING DISEASE-ASSOCIATED CELLS AND BIOMOLECULES: RECENT ADVANCES section. The corrected version was reposted on March 4, 2013.